TECHNISCHE UNIVERSITÄT MÜNCHEN
Fakultät für Medizin

Molecular mechanisms of the RIG-I mediated anti-tumor immunity

Diana Alexandra Kreppel

Vollständiger Abdruck der von der Fakultät für Medizin
der Technischen Universität München zur Erlangung einer Doktorin
der Medizinischen Wissenschaft genehmigten Dissertation.

Vorsitzender: Prof. Dr. Jürgen Ruland

Prüfer*innen der Dissertation:

1. Priv.-Doz. Dr. Hendrik Poeck
2. Prof. Dr. Dirk H. Busch
3. Prof. Dr. Julia Jellusova

Die Dissertation wurde am 29.07.2021 bei der Technischen Universität München eingereicht und durch die Fakultät für Medizin am 16.03.2022 angenommen.

Eidesstattliche Erklärung

Table of Contents

1. Abbreviations

3pRNA	5’ triphosphate double stranded RNA
AD	acidic transactivation domain
AIM2	absent in melanoma 2
AML	acute myeloid leukemia
AP-1	activator protein 1
APC	antigen-presenting cell
ASC	apoptosis-associated speck like protein containing a caspase recruitment domain
BCL10	B cell lymphoma 10
CARD	caspase recruitment domain
CD	cluster of differentiation
cGAS	cyclic GMP-AMP synthase
CpG	single-stranded DNA containing unmethylated CpG motifs
CLEC	C-type lectin domain
CLR	C-type lectin receptor
CTD	carboxy-terminal domain
CTL	cytotoxic lymphocyte
CTLA-4	cytotoxic T-lymphocyte-associated protein 4
DAMP	danger-associated molecular pattern
dsRNA	double-stranded RNA
DC	dendritic cell
ELISA	enzyme-linked immunosorbent assay
FACS	fluorescence activated cell sorting
FcRγ	Fc-receptor γ -chain
GFP	green fluorescent protein
HRP	horse raddish peroxidase
ICB	immune checkpoint blockade
IFN- α	Interferon-α
IFN-γ	Interferon-γ
IFNaR	Interferon- α receptor
IL	Interleukin
IRF	Interferon regulatory factor
ISD	interferon stimulatory DNA
ITAM	Immunoreceptor tyrosine based activation motif
LCMV	lymphocytic choriomeningitis virus
LF	lipofectamine
LGP2	laboratory of genetics and physiology 2
LN	lymph node
LPS	lipopolysaccharide
LRR	leucin rich repeat
MAPK	mitogen activated protein kinase
MAVS	mitochondrial antiviral-signaling protein
MDA5	melanoma differentiation-associated protein 5
MHC	major histocompatibility complex
MyD88	myeloid differentiation primary response 88

NFκB	nuclear factor kappa-light-chain-enhancer of activated B cells
NK cells	natural killer cells
NLR	NOD-like receptor
NOD	nucleotide-binding oligomerization domain
PAMP	pathogen associated molecular pattern
PD-1	programmed cell death protein 1
poly(dAdT)/dAdT	poly(deoxyadenylic-deoxythymidylic) acid
PEI	polyethyleneimine
p(I:C)	polyinosinic-polycytidylic acid
PRR	pattern recognition receptor
PYD	pyrin domain
RBC	red blood cell
RIG-I	retinoic acid-inducible gene-I-like receptors
RLR	RIG-I like receptor
siRNA	short-interfering RNA
SLR	stem-loop RNA
STING	stimulator of interferon genes
SYK	spleen tyrosine kinase
synRNA	synthetic dsDNA lacking 5'-triphosphate
TGF-β	transforming growth factor beta
TIL	tumor infiltrating lymphocytes
TIR	Toll/interleukin-1 receptor homology
TLR	Toll-like receptor
TNF-α	tumor necrosis factor-a
TNFR	tumor necrosis factor receptor
TRAF	TNFR-associated factor
TRIF	TIR-domain-containing adapter-inducing interferon-b
WNV	West Nile Virus

2. List of figures

3. Introduction

3.1. Innate and adaptive immune responses

Our immune system has evolved multiple layers of defense mechanisms to protect us against pathogens. Innate immune cells such as dendritic cells (DCs), granulocytes and macrophages distinguish self from foreign by germline encoded receptors which recognize common pathogen associated molecular patterns (PAMPS). Activation of these pattern recognition receptors (PRR) triggers a signaling cascade which immediately leads to immune cell activation, induction of inflammation or engulfment of pathogens by phagocytosis. Furthermore, PRR activation in dendritic cells allows their functional maturation and the initiation of an adaptive immune response through (i) the secretion of proinflammatory cytokines, (ii) presentation of processed peptides by major histocompatibility complex (MHC) molecules and (iii) engagement of costimulatory receptors on adaptive immune cells.

B and T lymphocytes of the adaptive immune system on the other hand apply a different strategy for host protection which involves the expression of antigen-specific receptors on the cell surface. The antigen receptor repertoire is highly diverse and therefore ensures protection against a plethora of potentially harmful substances. It is estimated that there are between $1x10^7$ – $1x10^9$ different B and T cell clonotypes in the human body [1]. T lymphocytes develop in the thymus whereas B lymphocytes mature in the bone marrow. After their development, each naïve T or B lymphocyte expresses a functional and unique T cell receptor (TCR) or B cell receptor (BCR), respectively. To ensure the absence of autoreactivity, adaptive immune cells are exposed to self-antigens during maturation and subsequently deleted if antigen receptor signaling is triggered. Lymphocytes travel through the body in anticipation of an event leading to activation of their unique antigen receptor with subsequent clonal expansion and differentiation into effector cells. B cells differentiate into plasma cells which secret further affinity maturated antibodies. CD4 T cells mature into different T helper cell subsets or regulatory T cells (T_{reg} cells) and CD8 T cells into cytotoxic effector cells.

The allocation of responsibilities is key for fast and robust but also long-lasting immunity. Hostile intruders and their byproducts threatening the host are immediately

recognized by PRR of the innate immune system which initiates a first line of defense. Through the subsequent activation of T and B lymphocytes our body mounts a highly specific immune response which includes the secretion of antibodies by plasma cells, activation of cytotoxic CD8 T cells and maturation of CD4 T helper cells into different effector subsets. The formation of memory B and T cells ensures long lasting immunity and fast expansion of antigen specific lymphocytes upon re-exposure. The trade-off for specificity and memory formation however is time – which is gained by immediate actions of innate immune responses.

3.2. Pattern recognition receptors

PRR are highly prevalent in our body and primarily utilized by innate immune cells such as dendritic cells and macrophages but a selection of PRR is also expressed by lymphocytes or nonimmune cells such as epithelial cells [2]. There are four groups of PRR: On the one hand Toll-like receptors (TLR) and C-type lectin receptors (CLR) which are membrane-associated receptors and on the other hand, NOD-like receptors (NLR) and RIG-I like receptors (RLR) which are located in the cytosol.

3.2.1. Toll-like receptors

While the majority of TLRs are expressed as surface receptors, TLR3, TLR7 and TLR9 are located intracellularly in endosome walls. Intracellular TLRs recognize viral and bacterial (or self) nucleic acids such as double-stranded (ds)RNA (TLR3), single-stranded (ss)RNA (TLR7) or unmethylated CpG motifs (TLR9). After ligand binding a signal cascade is initiated through adaptor proteins, most prominently myeloid differentiation primary response 88 (MyD88) which is an essential signaling component of all TLRs but TLR3 (which uses the adaptor protein TIR-domain-containing adapter-inducing interferon-b, TRIF). Downstream activation of interferon regulatory factors (IRF), particularly IRF3 and IRF7, induce antiviral immune responses and the production of type I Interferons (IFN-I) such as IFN-α or IFN-β. However, several other transcription factors can be activated. Important ones are the transcription factors of the nuclear factor kappa-light-chain-enhancer of activated B cell (NFκB) family and activator protein 1 (AP-1) which induce inflammation through the production of pro-inflammatory cytokines such as pro-interleukin (IL) IL-1β, IL-6 or TNF-α. (reviewed by [2] and [3])

3.2.2. C-type lectin receptors

The family of CLR comprises many different receptors characterized by their ability to bind different types of carbohydrates which are essential constituents of bacterial and fungal cell walls but also viruses. Most prominent members of the CTL family are Dectin-1 (C-type lectin domain family 7) and Mincle (Macrophage inducible calcium dependent lectin receptor) which bind to β-glucans and α-mannose respectively. CLR triggered signaling pathways are complex but often involve adaptor molecules with immunoreceptor tyrosin based activation motif (ITAM) such as Fc-receptor γ - chain (FcRγ) and converge to NFκB activation. Importantly, a fraction of CLR also crosstalk to TLR induced signaling pathways thereby modulating TLR induced cytokine production. For instance, the CLR CLEC4C inhibits TLR9 induced production of IFN-I and proinflammatory cytokines. TLR-induced production of IL-10 on the other hand is reinforced by CD209 (CLEC4L). Some CLR also recognize endogenous molecules released from dead cells. CLEC12A for instance binds uric acid crystals and dampens uric acid induced inflammatory responses [4]. CLEC9A on CD8 positive DCs on the other hand senses dead cells and induces SYK dependent cross-presentation of cell derived antigens to CD8 T cells [2], [5], [6].

3.2.3. NOD-like receptors

NLRs are located in the cytosol and involved in the detection of intracellular pathogens and endogenous molecules released from tissue injury, so called danger-associated molecular patterns (DAMPS) such as ATP or uric acid crystals. [2], [7].

NLR are subdivided into four families: NLRA, NLRB, NLRC and NLRP each with specific sets of effector domains. NOD1 and NOD2 belong to the NLRC subfamily and recognize peptidoglycans in the cell wall of bacteria. Receptor ligation leads to self-oligomerization and CARD dependent interaction with other CARD containing adapter proteins with subsequent NFκB and mitogen-activated protein kinase (MAPK) activation. NLR of the NLRP subfamily are important contributors to large, intracellular multiprotein complexes called inflammasomes. Inflammasomes are formed upon sensing danger signals and are crucial for the initiation of inflammation and induction of pyroptosis, an inflammatory variant of programmed cell death [8]. Inflammasome

activating signals are very diverse and include microbial derived molecules, ATP, particulate matters (uric acid, alum) and others and are mainly sensed by NLR. Upon oligomerization a crucial adaptor protein, apoptosis-associated speck like protein containing a caspase recruitment domain (ASC) bridges NLR ligation with caspase 1 activation. Caspase 1 cleaves precursor proteins of IL-1β, IL-18 and IL-33 and their secretion ultimately initiates an inflammatory response [7], [8].

3.2.4. RIG-I like helicases

RLH are cytoplasmatic PRR expressed in most cell types and are crucial for host defense against RNA viruses through robust induction of IFN-I and pro-inflammatory cytokines. In contrast to the endosome associated receptors TLR3, TLR7 and TLR9, RLH sense cytoplasmatic nucleic acids of virus infected cells. The RLH family comprises three members: retinoic acid-inducible gene-I-like receptor (RIG-I), melanoma differentiation-associated protein 5 (MDA5) and laboratory of genetics and physiology 2 (LGP2). Characteristic for all three RLH members is a central helicase domain and a carboxy-terminal domain (CTD). RIG-I is able to distinguish eukaryotic from foreign RNA through characteristic modifications of the 5'-triphosphate group after transcription in eukaryotic cells: an enzymatic addition of 7-methylguoanosin, which is also called "capping". The addition of 7-methylguoanosin takes place in the nucleus and since most RNA viruses propagate in the cytoplasm, viral derived RNA lacks a 5' cap. RIG-I is therefore considered a receptor for 5' triphosphate RNA (3pRNA) [9], [10]. For RIG-I activation 3pRNA binding to a complementary RNA strand is required [11].

Both MDA5 and RIG-I but not LGP2 have two N-terminal CARD domains for communication with downstream adaptor proteins. An important adapter protein of the RIG-I signaling cascade is mitochondrial antiviral-signaling protein (MAVS). MAVS is located in the membrane of mitochondria and also possesses a CARD domain which enables CARD-CARD interactions with RIG-I and MDA5. MAVS activates a signaling complex which consists of CARD9 and B cell lymphoma (BCL)10 to activate the canonical NFκB pathway leading to the production of IL-6 and the precursor cytokine pro-IL-1β. IL-1β maturation requires inflammasome activation and caspase-1 mediated cleavage of pro-IL-1β. This crucial step is initiated by RIG-I interactions with ASC and subsequent, MAVS and NLRP3 independent formation of an inflammasome [12].

Besides the production of pro-inflammatory cytokines, RIG-I/MAVS complexes also induce the production of type-I interferons, Interferon-α and Interferon-β, through tumor necrosis factor receptor (TNFR)- associated factor (TRAF)6 and IRF3. [2], [13]–[16].

As a consequence, virus induced RIG-I activation is translated into at least three different signaling pathways. Inflammation is induced through (i) MAVS dependent NFκB activation and secretion of IL-6 and pro-IL-1β and (ii) ASC dependent NLRP3 inflammasome activation with caspase-1 mediated production of IL-1β. Next, an effective anti-viral response is supported by (iii) MAVS dependent activation of IRF3 with concomitant production of type-I interferons [2], [17], [18].

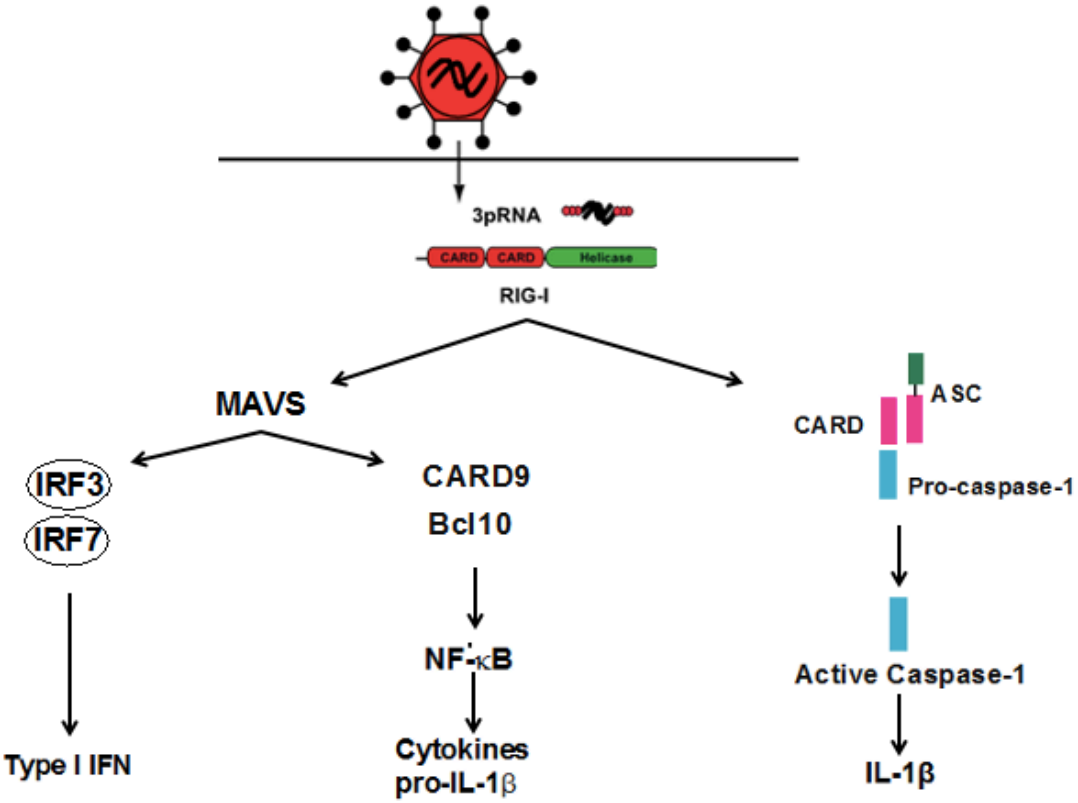

Figure 1: Recognition of RNA viruses and 3pRNA by RIG-I.

After 3pRNA ligation, RIG-I interacts with the adaptor protein MAVS. MAVS induces the transcription of type I interferon via IRF3 and 7 or proinflammatory cytokines via NFκB. MAVS-independent RIG-I induces the formation of the ASC-inflammasome for the generation of IL-1β. Adapted from [19].

3.3. Cytotoxic Immune Responses

Not only pathogens are targets of our immune system. Malignant cells are also considered 'non-self' and therefore sensed and eliminated by cytotoxic immune responses. Cellular cytotoxicity is primarily mediate through Natural-Killer (NK) cells and CD8 expressing cytotoxic lymphocytes (CTL). NK cells belong to the innate arm of the immune system and express a wide range of activating and inhibitory receptors which are necessary for effector functions and to recognize damaged, infected or malignant cells [20].

CD8 T cells require three extrinsic signals for proliferation and differentiation into effector cells (CTLs): (i) TCR mediated recognition of antigens coupled to MHC-I, (ii) costimulation of costimulatory cell surface receptors and (iii) uptake of cytokines such as type-I interferons or IL-12 [21]–[23]. As a result, CTLs release effector molecules such as IFN-γ and cell death inducing cytotoxins. To protect our body from T cell hyperactivation, T cells also express an array of regulatory cell surface receptors such as cytotoxic T-lymphocyte-associated protein 4 (CTLA-4) and programmed cell death protein 1 (PD-1) and receptor ligation dampens T cell mediated immune responses [24], [25]. This mechanism is also utilized by tumor cells to escape immune surveillance. Conversely, immune checkpoint blockade (ICB) of PD-1 and CTLA-4 strongly enhances tumor-directed immune responses. Comprehension of this mechanism paved the way for a plethora of successful clinical studies analyzing the benefit of so called "checkpoint inhibitor" treatments. [26]–[28].

CD8 TCR recognize antigens in conjunction with MHC-I, which is expressed by all nucleated cells. However, not every nucleated cell has the machinery to take up, process and present exogenous antigens via MHC-I. This unique property is referred to as "cross-presentation" and is usually carried out by specialized antigen-presenting cells (APCs) especially DCs. The functional maturation of DCs is critical for cross-priming and induction of adaptive antitumor immunity. Besides antigen-presentation by MHC-I and migration from tissue to regional lymph nodes (LNs) this also includes upregulation of costimulatory molecules such as CD80, CD86 as well as MHC-I/-II and the secretion of pro-inflammatory cytokines such as IL-6 or IL-12p40 [29], [30]. DC maturation alone can be achieved by a pro-inflammatory cytokine environment, which

however is insufficient for T cell activation and only results in the induction of T cell tolerance [31], [32]. Rendering DCs capable to elicit T cell differentiation into effector cells is referred to as DC licensing and classically achieved by interaction of DCs with T helper cells [33]. It has been shown that CD4 T cell help is dispensable for the induction of cross-priming in the presence of certain PRR stimuli in DCs, especially those inducing IFN-I [34].

3.4. PRR ligands as adjuvants for cancer therapy

Tumorigenesis and the immune system are closely linked. Inflammation plays a pivotal role in the initiation of malignancies, for example by promotion of angiogenesis through macrophages, facilitation of tumor spread and mechanisms to evade immune surveillance [35], [36].

Manipulation of the immune system is an emerging strategy for the treatment of malignancies. Immune checkpoint inhibition unleashes anti-tumor CD8 T cell responses and is becoming the mainstay of treatment of various advanced cancers [24], [25], [37]. But also the innate immune system is a potential target for tumor therapy. Especially for viral PRRs there is growing evidence that their signaling pathways can be hijacked to induce antitumor immunity:

Some immunogenic tumors can induce CD8 T cell priming against tumor antigens in humans, a mechanism that likely relies on sensing of tumor DNA by the host cyclic GMP-AMP synthase (cGAS)- stimulator of interferon genes (STING) pathway and is dependent on IFN-I [38]. Other patients without spontaneous induction of tumor infiltrating CD8 T cells have a less favorable prognosis [39], [40]. This patient group might benefit from therapies boosting an anti-tumor immune response, potentially by targeting the cGAS-STING pathway or other viral receptors. Our lab demonstrated previously that a systemic RIG-I agonist delayed progression of pseudo-lung metastasis of murine melanoma cells through initiation of an immune response but also direct effects on the tumor cells [41]. At the same time non-malignant cells expressing RIG-I were partly protected by upregulation of the survival protein BCL-x_L [42].

3.5. Objectives

3pRNA mimics a viral infection and activates RIG-I signaling pathways in dendritic cells and induces immunogenic cell death in tumor cells. The beneficial effect of 3pRNA/RIG-I activation in preclinical cancer models therefore likely is a combination of both effects. RIG-I signaling pathways in DCs have been described previously. Here we analyze the contribution of different downstream pathways in DCs to the induction of DC maturation and cross-priming of peptide-specific CD8 T cells in vitro and in vivo. Furthermore, we aimed to demonstrate cytotoxic capacity of the induced CD8 T cells in a prophylactic tumor model.

4. Material and Methods

4.1. Mice

Wild type C57/Bl6 mice were purchased from Janvier and mostly used at an age of 6 – 12 weeks for experiments. OT-I transgenic mice were purchased from Jackson laboratory. Genetically engineered knock-out mice for *Mavs*, *Asc*, *Ifnar1* and *Card9* were previously described [13], [43]–[45]. All mouse studies were performed according to guidelines approved by the Regierung of Oberbayern. Mice were housed in specific pathogen - free conditions at the Technische Universität München.

4.2. Regents for in vitro experiments

RPMI medium (Invitrogen) supplemented with 10% v/v FCS (Hyclone), 3 mM L-glutamine, 100 U/ml penicillin and 100 μg/ml streptomycin (Sigma-Aldrich) was used for in vitro experiments. OptiMEM reduced serum medium was purchased from Invitrogen. CFSE dye used to assess in vitro and in vivo proliferation was purchased from Invitrogen and used following the manufacturers recommendations. CpG 1826, poly (I:C) and LPS were purchased from Invivogen. ISD was purchased from Sigma-Aldrich as single strand oligonucleotides and was annealed by 30 min incubation at 75°C. Double stranded 3pRNA (sense, 5'-UCA AAC AGU CCU CGC AUG CCU AUA GUG AGU CG-3') was in vitro transcribed as previously described [41]. Control synthetic RNA (synRNA) was purchased from Eurofins (Ebersberg, Germany). However, the purity of in vitro transcribed 3pRNA stocks was variable resulting in partially inconsistent assays - especially as over the course of this study different

stocks were used in different experimental setups. Even though, as previously described the 3pRNA sequence does not include TLR7 activating motifs [41], contributions of other nucleotide-recognizing immunoreceptors to DC activation cannot be ruled out. This could explain why our negative control synRNA also showed modest immunostimulatory potential in some experiments despite the absence of a 5'-triphosphate group. Transfection of BMDCs was performed with Lipofectamine 2000 reagent (Life technologies). If not indicated differently, cells were transfected with ISD (3 μg/ml), 3pRNA (1 μg/ml), p(I:C) (1 μg/ml), poly dAdT (1 μg/ml) or synRNA (1 μg/ml). Alternatively, CpG 1826 was used at 0.075 μM and LPS at 20 ng/ml. For IL-1β secretion BMDCs were stimulated with LPS 50 ng/ml overnight followed by the addition of ATP (5mM; Sigma-Aldrich) 2 hours prior to analysis. Ovalbumin was purchased from Invivogen.

4.3. Generation of BMDC and in vitro stimulation experiments

For the generation of BMDC, mouse tibia and femur were flushed with 10-15 ml FACS buffer using a 23-gauge needle. Bone marrow cells were collected and filtered through a 100 μm cell strainer. Cells were transferred to a 15 ml canonical tube and centrifuged for 5 min, 350 – 400 g at 4°C. After RBC lysis for 5 min on ice, cells were washed with FACS buffer, pelleted and resuspended in RPMI medium supplemented with 10% FCS (v/v), 3 mM L-glutamine, 100 U/ml penicillin and 100 μg/ml streptomycin (sigma) and 20 ng/ml GMCSF (Immunotools, Germany). Cells were counted using a Neubauer counting chamber and 2.5 – 5 x 10^6 cells / 15 cm dish were cultured. Differentiation of BMDCs with GMCSF results in a relatively heterogeneous population of DCs, macrophages and neutrophils, as GMCSF stimulates the differentiation of all three lineages [46]. We minimized the number of granulocytes in the culture by regularly exchanging parts of the supernatant with fresh medium and thus removing all non-adherent cells including granulocytes. On day 7 of bone marrow culture the loosely attached DCs were gently flushed from culture plates with the objective not to release macrophages that are firmly adherent to the plate [46]. BMDCs were subsequently used for in vitro stimulation experiments. For purification of CD8 lymphocytes used for coculture assays, MACS beads were used (Miltenyi biotech) and cells were purified following the manufacturers recommendations. For coculture experiments in 96 Well plates 25 000 BMDCs were incubated with peptide (OVA, 1 μg/ml) and stimulus for 1

day and subsequently cultured with 100 000 CD8 T lymphocytes for 2 - 3 days. Proliferation was assessed by FACS [47]. To assess cytotoxicity in vitro, the murine T cell lymphoma cell line EL-4 was utilized. Target cells were pulsed with 1μM SINFEKL peptide for 30-60 min at 37°C and subsequently labeled with 0.2 μM CFSE. Non-target cells were stained with 2 μM CFSE. Next, 10 000 cells were added at a 1:1 ratio to in vitro BMDC/OT-I co-cultures and incubated for 4 hours. Magnitude of killing was calculated using the formula 100 - (sample $CFSE^{low}$/sample $CFSE^{high}$)/control $CFSE^{low}$/control $CFSE^{high}$).

To obtain splenic DCs MACS beads were used (Miltenyi biotech) and cells were purified following the manufacturers recommendations. Splenic DCs were stimulated as described above for BMDCs, however OVA was used at a concentration of 6.7 μg/ml and the incubation of DCs with OT-I cells was 3 days instead of 2 if not otherwise indicated.

4. 4. Cytokine quantification by ELISA

Commercially available ELISA kits were purchased from ebioscience, BD Biosciences, or R&D systems and performed following the manufacturers recommendation. Briefly, 96 well flat bottom plates (Nunc®) were coated with 100 μl of diluted capture antibodies and incubated overnight at 4°C. After aspiration of wells and five times washing with washing buffer containing 0.05% Tween-20, wells were blocked with 250 μl 5% w/v milk powder or 5% w/v BSA for ≥ 1 hour at room temperature on a shaker. After aspiration and five times washing standard protein dilution and cell supernatant were added and plates were incubated overnight at 4°C on a shaker. Supernatants were aspirated, wells washed for a total of five times and horse radish peroxidase (HRP)–labeled detection antibody added. After incubation for ≥1 hour at room temperature, wells were washed again 5 times, HRP substrate was added and plates were incubated at room temperature in the dark. The reaction was stopped by adding 2N H_2SO_4 stop solution and the plate was immediately read on an ELISA reader at 450 nm. A standard curve with at least seven 1:2 serial dilutions was run on each ELISA plate. Concentrations of target antigens were quantified by calculating the mean absorbance for each condition and standard and subtracting zero absorbance of the standard. The standard curve was plotted in Microsoft excel and unknown

concentrations were calculated using their absorbance values and known concentration from the standard.

4.5. In vivo Immunization Experiments

Stimulation of adoptively transferred OT-I cells (adopted from [48]): One day before vaccinations 3 x 10^6 CFSE labeled splenocytes from OT-I mice were injected into the tail vein of experimental animals. One day later 3 μg OVA (or as indicated in figures) together with 25 μg 3pRNA or 25 μg p(I:C) (complexed in 3.5 μg in vivo-JetPEI from Polyplus) or 15 μg CpG were injected intravenously (I.V.). Three days after vaccination animals were sacrificed and splenocytes analyzed with Flow cytometry for proliferation and intracellular IFN-γ or cultured with OVA 50 μg/ml for 1 day for analysis of IFN-γ secretion by ELISA.

For the stimulation of endogenous OVA specific CD 8 T cells, mice were injected on day 1 subcutaneously (S.C.) into the hindleg with OVA and stimuli (concentrations as described above). On day 7 treatment was repeated and on day 12 splenocytes and cells from the regional lymph node (popliteal LN) were restimulated in vitro with OVA 1 μg/ul for 3 days and then analyzed by Flow cytometry and ELISA as described above.

To assess in vivo cytotoxicity, mice were injected S.C. or I.V. with PBS, OVA 30 μg, 3pRNA 25 μg (complex with jetPEI), p(I:C) 25 μg (complexed with jetPEI) or CpG 3nM on day 0. Splenocytes from syngeneic donor mice were pulsed with SIINFEKL (2 μM) and labeled with CFSE (0.2 μM), mixed 1:1 with splenocytes without SIINFEKL which were stained with CFSE 2 μM and injected I.V. in the experimental animals on day 6. On day 7 mice were sacrificed and target cell frequencies in the spleen analyzed as described for in vitro experiments.

4.6. Mouse dissection and flow cytometry of single cell suspensions

Mice were euthanized by isoflurane overdose and cervical dislocation. Lymphatic tissue of interest such as spleen and lymph nodes were extracted and fat removed. Tissues were grinded through a 100 μm cell strainer with a plunger, cell strainers were washed with 3 ml FACS buffer (1 x PBS + 1% FCS) and suspensions were additionally filtered through a 70 μm cell strainer. Cells were transferred to a 15 ml canonical tube and pelleted by centrifugation at 350 g for 5 min at 4°C. Pellet was resuspended in 5

ml 1 x red blood cell (RBC) lysis buffer (ebioscience) and incubated on ice for 5 minutes. After washing with 10 ml FACS buffer, cells were pelleted again, resuspended in 2 – 10 ml FACS buffer (depending on organ of interest) and cell counts were determined using a Neubauer counting chamber and trypan blue. At least 1.0 x 10^6 cells per flow cytometry stain were transferred to a 96-well v-bottom plate. After centrifugation for 5 minutes, 350 – 400 g at 4°C, supernatant was poured and cells were resuspended in 50 µl anti-CD16/CD32 (BD, 2.5 µg/ml; 'Fc-block') in FACS buffer and cells were incubated for 30 minutes at 4 - 8°C. Cells were washed with 200 µl FACS buffer and incubated in 50 µl FACS buffer with diluted fluorophore-coupled monoclonal antibodies for 30 minutes at 4 - 8°C. Intracellular cytokine stainings were performed using the Foxp3 transcription factor staining kit (ebioscience) following the manufacturers recommendations. Cells were first re-stimulated in vitro with PMA (50 ng/ml) and Ionomycin (1 µg/ml) in the presence of 1x Monensin (ebioscience) stained overnight at 4°C in permeabilization buffer. Samples were acquired on a BD Canto II flow cytometer. Additional single stain controls were recorded to generate a compensation matrix. FACS files were analyzed with FlowJo (Treestar). For flow cytometric cytokine quantification the Mouse Th1/Th2/Th12 Cytokine Kit from BD Bioscience was used according to the manufacturer's recommendations.

4.7. B16 tumor model

B16 murine melanoma cells expressing ovalbumin (B16-OVA) were cultured in DMEM medium supplemented with 10% v/v FCS (Hyclone), 3 mM L-glutamine, 100 U/ml penicillin and 100 µg/ml streptomycin (Sigma-Aldrich) and 400 µg/ml G418 (Sigma-Aldrich). Cells were harvested and cell concentration determined using a Neubauer counting chamber. 15 x 10^3 – 1,5 x 10^6 cells resuspended in 200 µl PBS were subcutaneously injected into the flank of wild-type C57Bl/6 mice. Mice were sacrificed when the tumor diameter exceeded 1.5 cm or adverse events occurred such as tumor ulceration. In a prophylactic setting, mice were immunized with 3 µg OVA or OVA + 3pRNA (at 15 or 25 µg/ml) complexed in jetPEI on day 0 and 14 followed by S.C. B16-OVA injection on day 19 or they were vaccinated on day 0 only followed by tumor challenge on day 14.

4.8. Statistics

Statistical calculations were performed with Prism software (GraphPad). If not stated otherwise two tailed student t-tests were used for the comparison of two groups or the one way ANOVA test with Bonferroni posttest for multiple groups. Statistical significance was set at $p < 0.05$, <0.01, <0.001 and <0.0001 and indicated by asterixis (*, **, *** and **** respectively).

5. Results

5.1. Consequences of RIG-I ligation in DCs in vitro

5.1.1. RIG-I activation induces maturation of DCs

As a model to study DC activation we used bone marrow derived dendritic cells (BMDCs) as described previously [46]. To assess the effect of RIG-I ligation on DC activation, we transfected BMDCs with the RIG-I ligand 3pRNA in titrated doses (0.1 - 1.5 μg/ml) and stimulated cells overnight. The next day, upregulation of costimulatory molecules was assessed by flow cytometry. We detected enhanced expression of the B7 family members CD80 and CD86 as well as upregulation of MHC-I and MHC-II molecules. DC activation with 3pRNA was dose-dependent and peaked at a concentration of 1 μg/ml, which is the concentration that was used for future in vitro experiments. Upregulation of activation markers is displayed as fold increase compared to base-level expression of unstimulated samples (Fig.2A).

We next sought to compare DC activation by 3pRNA with other known stimulants. As controls, cells were either transfected with dsRNA lacking the 5'-triphosphate (synRNA) or stimulated with TLR agonists CpG (TLR9), LPS (TLR4) or agonists of cytosolic nucleic acid sensing receptors (p(I:C) – MDA5, ISD – cGAS, dAdT – AIM2). All of the tested PRR ligands enhanced expression of CD80 and CD86 indicating DC maturation. At the same concentration (1 μg/ml) 3pRNA was more potent than the other tested cytosolic PRR ligands (Fig. 2B). The two negative controls, the transfection agent lipofectamine and synRNA, showed no significant induction of the examined cell surface markers (Fig. 2B).

We measured accumulation of pro-inflammatory cytokines in the supernatant of in vitro stimulated BMDCs by ELISA. RIG-I ligation resulted in the secretion of (1) pro-inflammatory cytokines such as IL12-p40 and IL-6, (2) IFN-α as well as (3) IL-1β (Fig. 2C). IL-12p40 secretion was lower compared to TLR stimulated samples (CpG: 21394.6 µg/ml and LPS: 9240.3 µg/ml) (Fig. 2C). This finding is in line with data published by Negishi et al in 2012 [49], showing that the cytokine gene profile induced by RLR in peritoneal macrophages is dominated by IFN-I, whereas TLR ligands preferentially induce the transcription of IL-12. IL-6 was similarly less induced by 3pRNA compared to LPS and CpG (Fig. 2C). SynRNA did not induce relevant amounts of any of the tested cytokines. RIG-I ligation also resulted in the secretion of IL1-β. However, with an average of 73.4 pg/ml in our experiments, the amount of IL-1β was lower compared to the level achieved by the AIM2 stimulus dAdT (241.9 pg/ml) or LPS+ATP (4913.0 pg/ml) (Fig. 2C). Altogether this data confirms activation of three pathways downstream of RIG-I namely (1) NFκB [13], [14] (2) IRF3/7 [13], [14] and (3) ASC inflammasome activation [12].

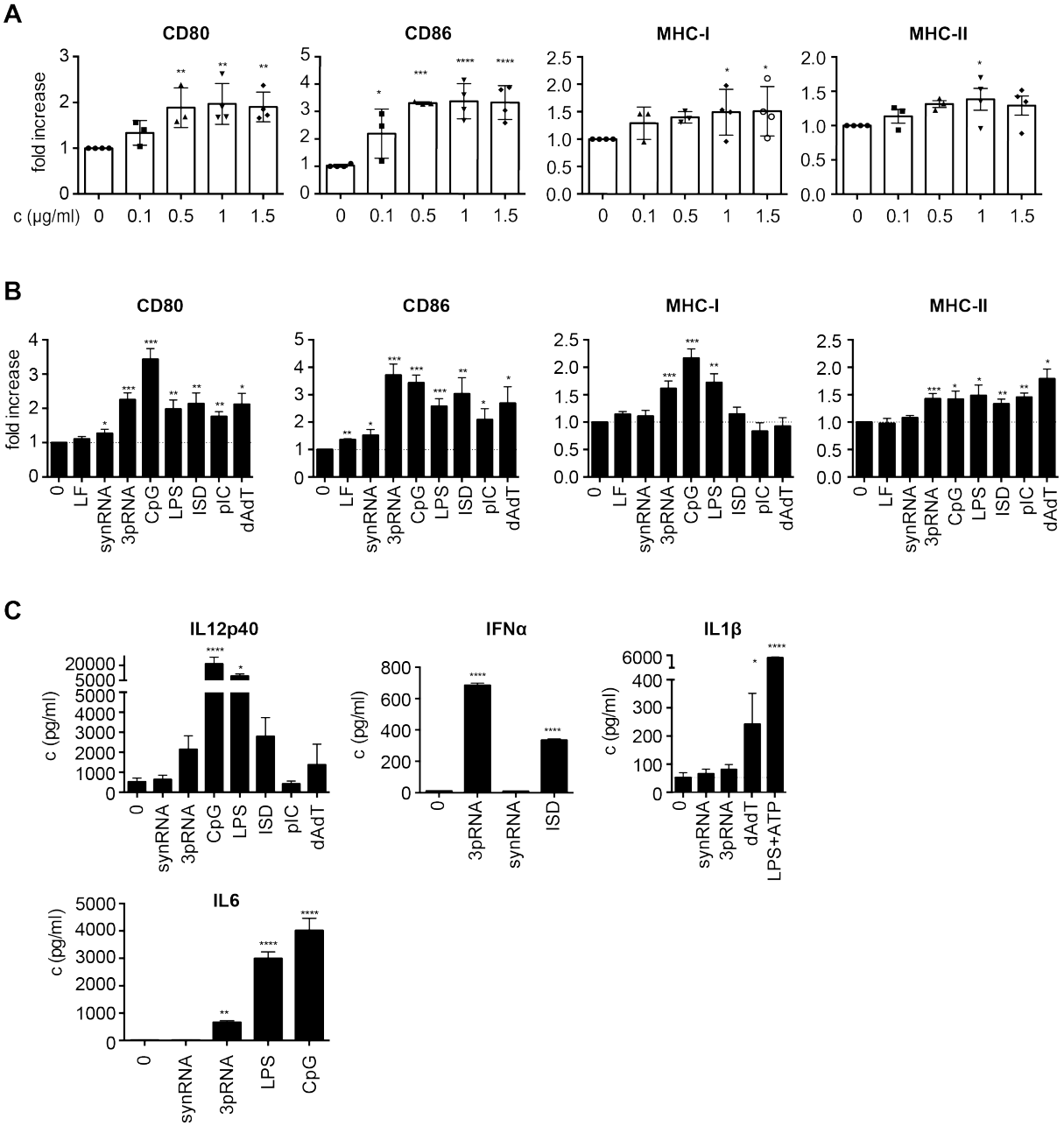

Figure 2: 3pRNA induces upregulation of costimulatory molecules and cytokine secretion in BMDCs.

*(A,B) Column charts show expression of indicated surface marker on BMDCs after overnight stimulation with (A) titrated 3pRNA dose (0.1 – 1.5 µg/ml) or (B) indicated stimuli (synRNA, 3pRNA, pIC and dAdT at 1 µg/ml, ISD 3 µg/ml, CpG 0.075 mM and LPS at 20 ng/ml), as determined by flow cytometry. Expression levels were depicted as MFI (mean fluorescence intensity) normalized to unstimulated control ("0"). Columns indicate mean fold increase and each data point represents n=1, data were pooled from at least 3 independent experiments. Error bars in (A) indicate SD and in (B) SEM. (C) Charts show mean amount of the secreted cytokine IL-12p40, IFNα , IL-1β, and IL-6 in the supernatant of BMDC cultures after overnight stimulation with indicated stimuli. Cytokine secretion was assessed by ELISA. Error bars indicate SEM. Data was pooled from at least 3 independent experiments for IL-12p40, from at least 2 independent experiments for IL-1β. IFNα data was pooled from technical duplicates in 1 experiment. IL-6 data is representative for 2 independent experiments, data was pooled from technical triplicates. Statistical significance was determined by one way ANOVA. * p < 0.05; **, p < 0.01, ***, p < 0.001; ****, p < 0.0001.*

As the differentiation of bone marrow cells with GMCSF only generates cells with morphologic and functional features of DCs, but remains an artificial model, we verified

our observations with freshly isolated mouse splenic DCs. MACS purification of splenic DCs resulted in on average 90.5 % CD11c+ cells among all live cells, 24.1% of which were CD8α+ (Fig. 3A), a DC subset known to be particularly capable of cross-presenting exogenous antigens [50]. In line with our GMCSF DC model, splenic DCs upregulated CD86 in response to RIG-I ligation or control stimuli (Fig. 3B). On day 8 of our bone marrow in vitro culture CD11c expression was similarly high although as demonstrated by Singh-Jasuja et al [51] activated DCs slightly downregulate CD11c which in our experiments was most prominent in 3pRNA stimulated samples compared to control stimuli (3pRNA 67.7%, unstimulated 80.1% CD11c+) (Fig. 3C). Next we compared CD86 expression using two different gating strategies and found that CD86 was similarly expressed on the cell surface irrespective of the gating strategy (CD11c+ vs. all live cells) (Fig. 3D). As the majority of GMCSF cultured cells are CD11c+ and the response to stimulation is identical in CD11c+ cells and all live cells (Fig. 3C, D), we limited FACS analysis in future experiments to the detection of size (FSC-A), granularity (SSC-A), viability and the maturation markers CD80 and CD86 as well as MHC-I and -II.

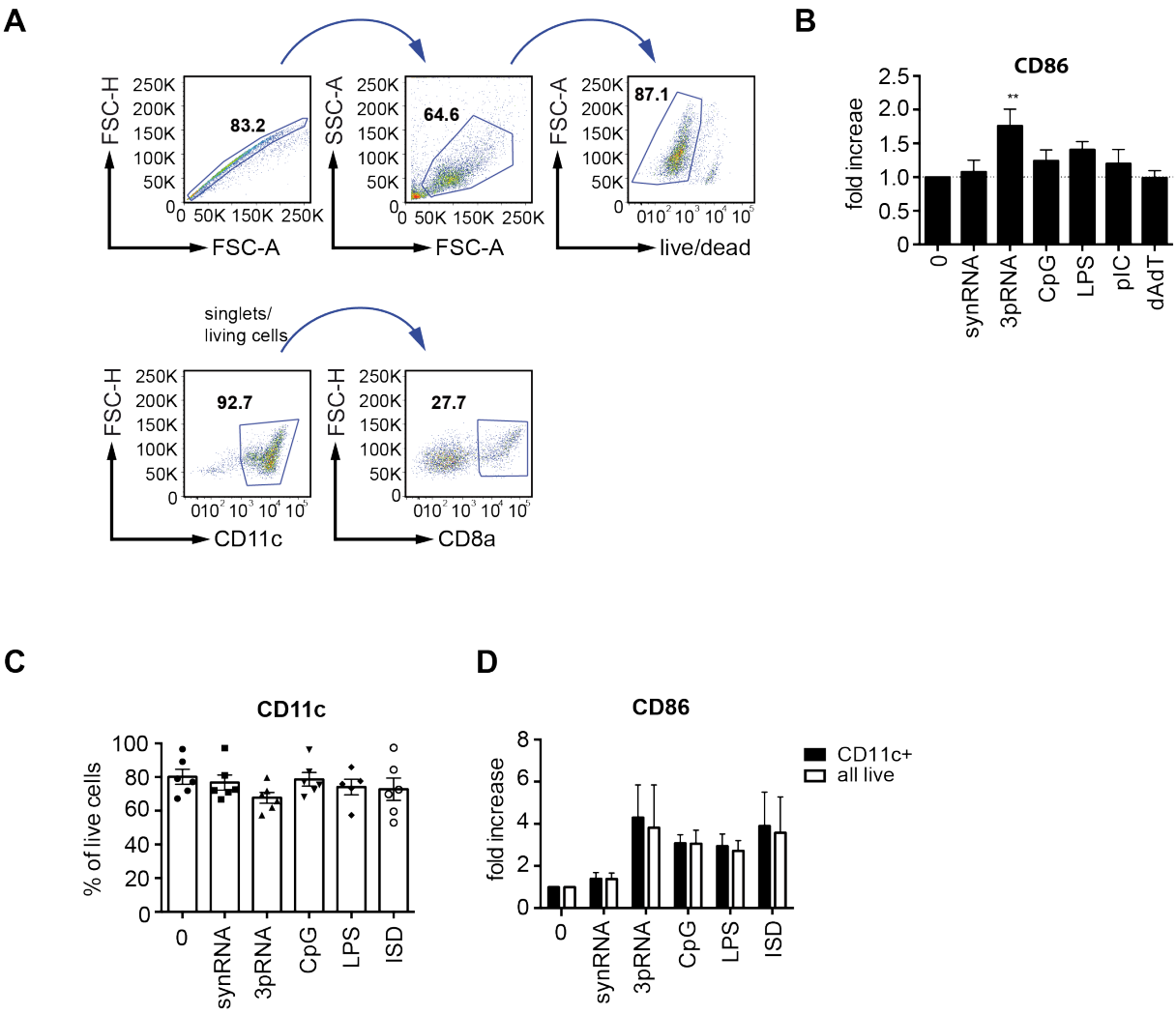

Figure 3 CD11c expression and upregulation of CD86 on splenic dendritic cells.

*(A) Representative flow cytometry dot plots show gating strategy for splenic dendritic cells (representative for n=4 in at least 3 independent experiments). (B) Bar charts show fold increase of surface CD86 after overnight stimulation with indicated stimuli. Columns indicate mean values and error bars standard deviation. Data was normalized to unstimulated control ("0"). (C) Graph shows mean percentage of CD11c expressing live splenocytes after overnight culture with indicated stimuli. Each data points represents n=1, data was pooled from at least 3 independent experiments. Error bars show SEM. (D) CD86 MFI mean fold increase (compared to unstimulated control) was determined by flow cytometry after overnight stimulation with indicated stimuli. CD86 expression on splenic DCs was assessed by either gating on all live DCs or CD11c positive DCs. Error bars indicate SEM. Shown data was pooled from at least 3 independent experiments. Statistical significance was determined by one way ANOVA **, $p < 0.01$.*

Taken together the differentiation of bone marrow cells with GMCSF is an effective method to generate large amounts of CD11c+ DCs [46] and we show that these BMDCs are similar to splenic DCs in their reaction to adjuvants in vitro. Our findings suggest that BMDC stimulation with 3pRNA induces their maturation as indicated by upregulation of costimulatory molecules and the secretion of pro-inflammatory cytokines such as IFNα, IL1-β and IL-12p40.

5.1.2. DC activation via RIG-I is mediated by MAVS and IFNaR, but is independent of CARD9 and ASC signaling

Expression of costimulatory surface proteins and MHC molecules (especially MHC-I) are known to be strongly enhanced by interferons [52], [53]. Seth et al demonstrated that RIG-I recruits the adaptor protein MAVS to transduce the signal to IRF3/7 for IFN-I expression and activates the transcription factor NFκB [13]. Interferons can be taken up by DCs via interferon-α/β receptor 1(IFNaR1). Thus, we hypothesized that MAVS and autocrine stimulation of IFNaR1 potentially play a crucial role in RIG-I induced DC maturation.

BMDCs deficient for MAVS, CARD9, ASC, IFNaR1 or wild-type (WT) DCs incubated with anti-IFNaR1 blocking antibody, were stimulated overnight with 3pRNA or the indicated PRR ligands as controls. Combined data of at least three independent experiments suggest that the expression of all four examined cell surface molecules was abolished in 3pRNA stimulated $MAVS^{-/-}$ BMDCs whereas - as expected - DC maturation induced by the MAVS independent PRR ligands CpG, LPS, ISD and dAdT was not impaired (Fig. 4A). Figure 4B shows representative histogram plots of stimulated MAVS deficient versus wild-type DCs.

MAVS is the central adaptor protein in the RIG-I signaling cascade and also transduces the signal to CARD9 which subsequently activates NFκB transcription factors for the initiation of a pro-inflammatory cytokine milieu [12]. Confirming already published data, IL-12p40 and IL-1β secretion was significantly decreased after 3pRNA stimulation in the absence of MAVS: from 7.5-fold compared to the unstimulated sample to 1.7 (IL-12p40) and from 2.1 to 1.2 (IL-1β) respectively (Fig. 4C).

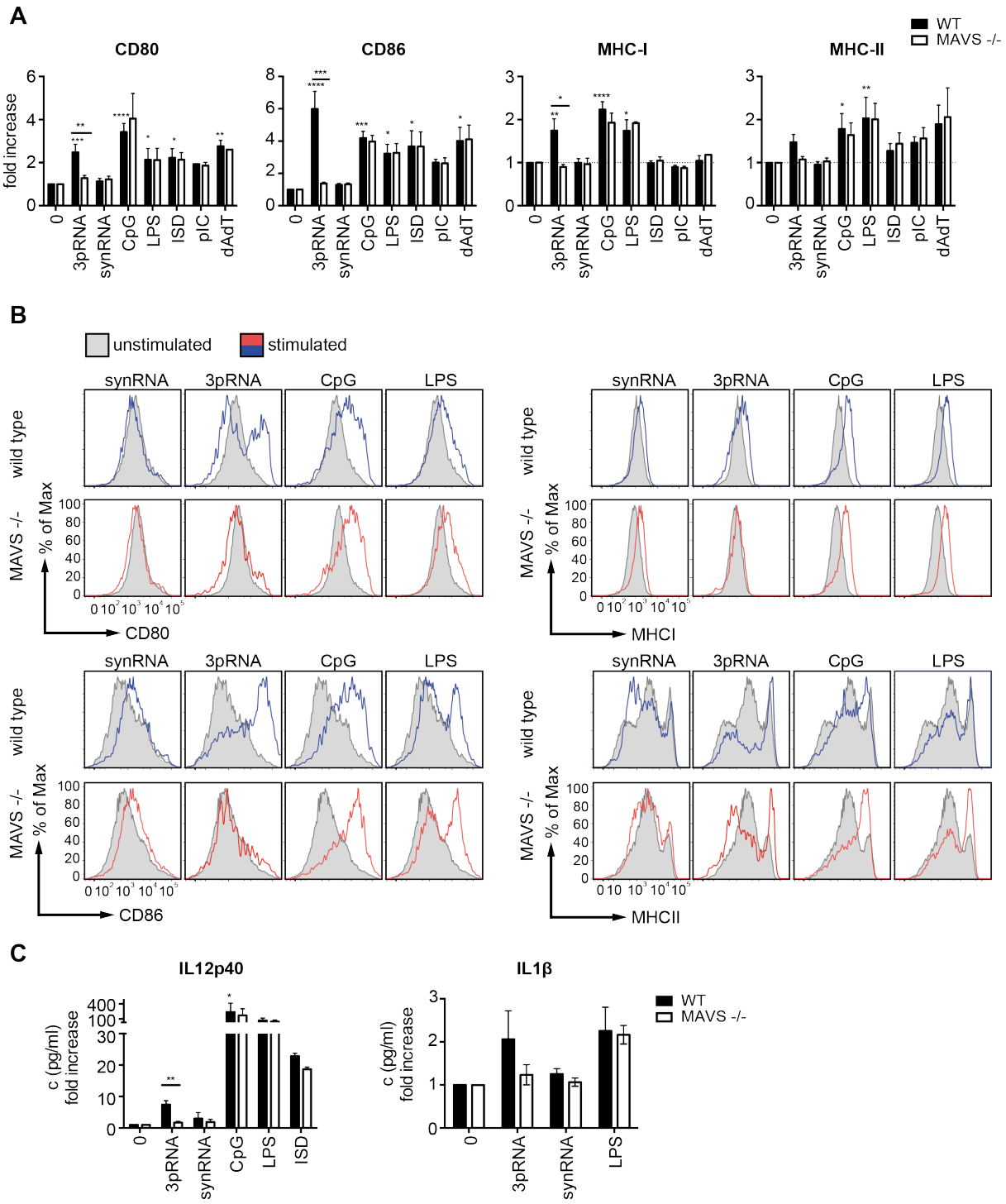

Figure 4: 3pRNA mediated upregulation of costimulatory molecules and cytokine secretion of BMDCs is MAVS dependent.

*(A) Wild-type (black columns) or MAVS deficient (white columns) BMDCs were stimulated in vitro with indicated stimuli and upregulation of CD80, CD86, MHC-I and MHC-II was determined by flow cytometry. Columns show mean fold increase of MFI, normalized to unstimulated control ("0"). Error bars indicate SEM. Data was pooled from n=2-5 in at least 2 independent experiments (B) Representative histogram plots show upregulation of CD80, CD86, MHC-I and MHC-II on wild-type (blue) or MAVS deficient (red) BMDCs. Grey histogram represents unstimulated control samples. Cells were stimulated overnight as indicated. (C) Secretion of IL-12p40 and IL-1β into the supernatant of stimulated samples was determined by ELISA. BMDCs were either derived from wild-type (black columns) or MAVS deficient (white columns) mice. Data was pooled from at least 3 independent experiments (except for ISD which is n=2). Statistical significance was determined by students t-tests for comparison of 2 groups and one way ANOVA for multiple comparisons. * p < 0.05 **, p <0.01 ***, p < 0.001 ****, p < 0.0001.*

Next we examined the role of the two downstream pathways of MAVS (IRF3/7 - IFN I and CARD9 - NFκB) in the regulation of costimulatory molecules and MHC expression. We found CD80/-86 and MHC-I/-II upregulation in response to 3pRNA to be almost abrogated in BMDCs with genetically deficient IFNaR1 signaling (Fig. 5A). Furthermore, antibody blockade of type I interferon receptor in 3pRNA stimulated samples had a similar effect and decreased expression of all four analyzed cell surface markers almost to the baseline (Fig. 5B). The PRR ligand ISD that is known to predominantly induce IFN-I [54], [55], but also CpG displayed a severely reduced capability to mature DCs when IFNaR1 signaling was impaired (Fig. 5A).

In contrast, FACS analysis of ASC and CARD9 deficient BMDCs showed an unchanged DC maturation. Upregulation of CD80, CD86, MHC-I and MHC-II after stimulation with 3pRNA and all tested TLR ligands was not altered compared to WT BMDCs (Fig. 5C and 5D). Our results outline the critical role of IFN-I for RIG-I induced BMDC maturation and the key role of MAVS and IFNaR in this process.

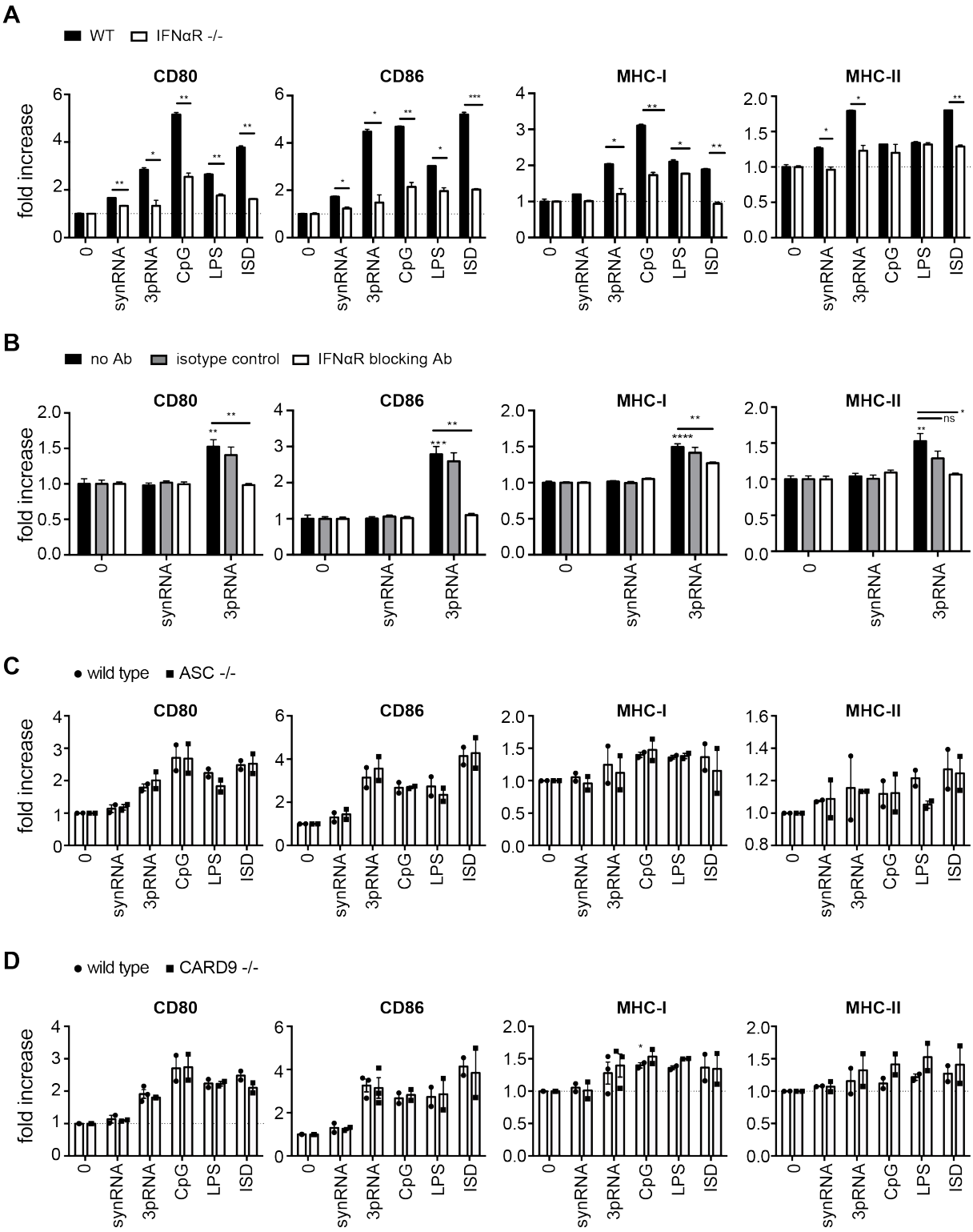

Figure 5: Type 1 interferon signaling but not ASC or CARD9 is essential for RIG-I mediated BMDC maturation in vitro.

(A) BMDCs from wild-type (black columns) or IFNaR knock-out mice were stimulated overnight in vitro as indicated and upregulation of costimulatory surface markers measured by FACS. Shown are normalized mean MFIs with negative control set to one. Data was pooled from 2 independent experiments and 2 mice per genotype. (B) Wild-type BMDCs were incubated with a monoclonal anti-IFNaR blocking antibody (white columns) or isotype control (grey columns) before stimulation with either 3pRNA or synRNA. Mean fold increase of costimulatory molecules was normalized to unstimulated samples. Data was pooled from technical triplicates in 1 experiment. (C, D) BMDC in vitro cultures from wild-type (dots) and either (C) ASC deficient or (D) CARD9 deficient C57BL/6 mice (squares) were stimulated overnight as indicated. Expression of CD80, CD86, MHC-I and MHC-II was normalized to unstimulated control. Each data point represents an in vitro culture of one individual mouse. Columns represent mean values ± SEM in A-D. Statistical significance was determined by students t-

*tests for comparison of 2 groups or one way ANOVA for multiple comparisons. * p <0.05; ** p < 0.01, *** p < 0.001, **** p<0.0001.*

5.2. Analysis of RIG-I mediated cross-priming of CD8 T cells in vitro

5.2.1. RIG-I activation in BMDCs and splenic DCs induces activation of peptide specific CD8 T cells

After having shown that RIG-I ligation induces the upregulation of costimulatory molecules and the secretion of cytokines, we next asked whether RIG-I activation also renders DCs competent to prime CD8 T cells. To assess the capacity of RIG-I stimulated DCs to cross-prime naive CD8 T cells, we transfected BMDCs with 3pRNA and additionally incubated the cells with the model antigen chicken egg ovalbumin (OVA). After overnight stimulation we cocultured the cells with CFSE-labeled OVA specific TCR transgenic CD8 T cells from OT-I mice. CD8 T cell activation was determined by T cell proliferation (CFSE-dilution assessed by flow cytometry and 'proliferation' defined as fraction of cells that divided at least once [47]). CD8 effector function was assessed by IFN-γ production and secretion (by flow cytometry and ELISA respectively and in vitro cytotoxicity.

To establish this in vitro model, we first tested immunogenicity of OVA protein itself (Fig. 6A, B). Coculture of BMDCs and OT-I cells with increasing OVA concentrations in the culture medium showed that higher OVA concentrations are immunogenic enough to activate CD8 T cells without the addition of an adjuvant. Only the OVA concentration of 1 µg/ml allowed the induction of a significant adjuvant effect by the addition of 3pRNA (Fig 6A). OVA alone also stimulated cocultured OT-I cells to release small, but detectable amounts of IFN-γ. However, in contrast to OVA induced OT-I expansion, IFN-γ secretion was strongly enhanced after the addition of 3pRNA to any of the tested OVA concentrations (Fig. 6B). Due to the immunogenic effect of higher OVA concentrations, particularly on OT-I cell proliferation, we used the lowest tested OVA concentration, 1 µg/ml, for future coculture experiments.

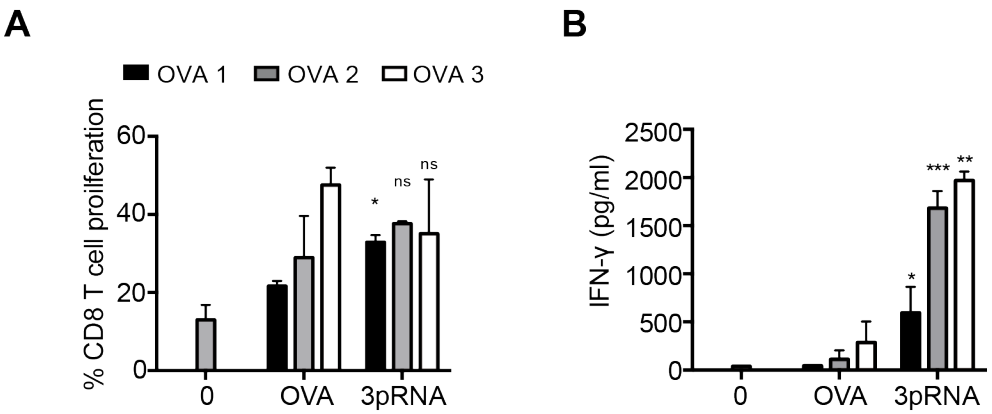

Figure 6: OVA dose dependent cross-priming of CD8 T cells in coculture assays.

*(A) BMDCs and CFSE labeled OT-I cells were cocultured in the presence of increasing OVA concentrations (OVA1-3 = 1 to 3 µg OVA/ml respectively,) ± 3pRNA 1 µg/ml. Y-axis indicates OT-I proliferation and represents the fraction of cells that have undergone at least one cell division (as percentage of total live CD8 T cells). (B) IFN- γ was measured in the supernatant of cocultured cells by ELISA. Cells were stimulated as in (A). Columns show mean values + SEM. Data was pooled from technical duplicates of one experiment. Statistical significance was determined by one way ANOVA for multiple comparisons (OVA vs 3pRNA with same OVA concentration) *p < 0.05; ** p < 0.01, ***p < 0.001; ns, not significant.*

Next we examined whether OT-I activation in our in vitro assay follows the immunologic principles of antigen cross-presentation by DCs and antigen-specific activation of CD8 T cells. All tested PRR ligands induced marked proliferation and IFN-γ release in OT-I cells cocultured with DCs and OVA. Proliferation as well as cytokine secretion were abrogated when (1) DCs and T cells were incubated without OVA or when (2) OT-I cells were stimulated directly without DCs in the culture (Fig. 7A-C). The first observation - no OT-I proliferation and IFN-γ secretion in cultures without OVA - proofs that OT-I activation through 3pRNA is peptide dependent. Additionally, the fact that OT-I cells could not be directly stimulated by OVA (at a concentration of 1µg/ml) and 3pRNA confirms that OVA has to be processed by DCs and presented to OT-I cells. Next, IFN-γ secretion and OT-I T cell proliferation also correlated with the 3pRNA dose: at a concentration of 1 µg/ml the adjuvant effect of 3pRNA peaked and increased OT-I proliferation by 6.1-fold and IFN-γ release by 15.5-fold compared to OVA alone (Fig. 7D, E)

To further assess functionality of activated OT-I cells, we assessed their capacity for peptide specific target-cell lysis (Fig. 7F, G): For this, BMDCs were stimulated in the presence of OVA and cocultured with naive OT-I cells as described above (with one modification: 10 µg/ml OVA instead of 1 µg/ml were used). Subsequently two populations of EL-4 cells (a C57BL/6 derived T cell lymphoma cell line) were added to

the samples: target cells and non-target cells. Target cells were pulsed with SIINFEKL, the immunogenic peptide of OVA, and stained with a low concentration of CFSE. Non-target cells were not treated with SIINFEKL but labeled with a high CFSE concentration. After four hours incubation the frequencies of CFSE-labeled cells were analyzed by flow cytometry. Pooled data of at least 3 independent experiments show that 3pRNA induced potent CTLs that kill on average 62.1% of their target cells and thus are 5.6 times more effective CTLs than OT-I cells in samples incubated with OVA, but without an adjuvant (Fig. 7F, G). RIG-I ligation elicited the most robust cytotoxic response (fold increase of specific lysis 3pRNA: 5.6, CpG: 3.4, LPS: 4.1) although CpG and LPS stimulation exceeded 3pRNA at the tested concentration with regard to OT-I proliferation and secretion of IFN-γ (Fig. 7A-C).

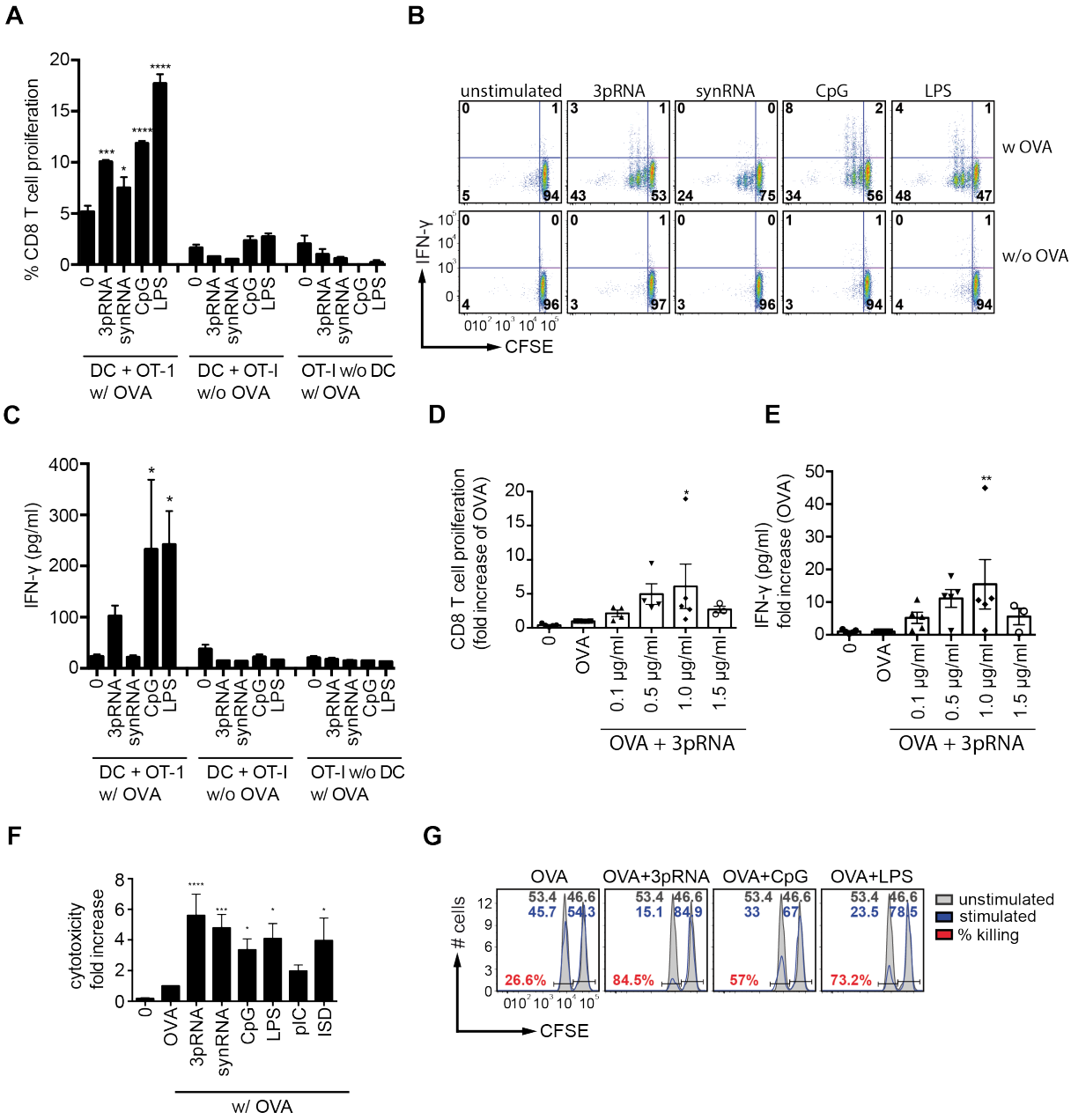

Figure 7: 3pRNA-RIG-I signaling in BMDCs induces OT-I priming and lysis of target cells.

For coculture experiments BMDCs were incubated for 1 day with or without OVA and with or without adjuvant. Then CFSE labeled OT-I cells were added to the culture for another 2 days. Then Proliferation, IFN-γ and peptide specific killing was assessed. (A) In addition to the general setup for cocultures some samples did not include DCs to show the effect of adjuvants and OVA on OT-I cells. The fraction of "CFSE negative" OT-I cells (cells that had undergone at least one cell division) was measured by flow cytometry. Shown are mean values with SEM of technical duplicates or triplicates. This experiment is representative of n=3 in 3 independent experiments. (B) Representative flow cytometry plots show CFSE labeled OT-I cells after 2 day coculture with wild-type BMDCs with or without OVA and stimulated as indicated. Cells were additionally stained intracellularly with a monoclonal antibody against IFN- γ. (C) BMDCs and OT- I cells were cocultured as in (A) and stimulated as indicated. After 2 day culture IFN- γ was measured in the supernatant by ELISA. Columns show mean IFN- γ concentrations and SEM. Data shows pooled data of n=2 in 2 independent experiments for DC+OT-I+OVA +/- adjuvant and n=1 in 2 experiments (thawed cells) for the other settings. (D, E) BMDC and OT-I cocultures were incubated in vitro with OVA ± increasing 3pRNA concentrations ranging from 0.1 – 1.5 µg/ml. (D)OT-I proliferation was determined by CFSE dilution. (E) IFN- γ secretion into the supernatant was assessed by ELISA. Columns indicate mean values and each data point represents n=1. Data were pooled from at least 3 independent experiments (F) Cocultures were set up as described above. On day 2 of coculture target cells were added to the samples which were either pulsed with SIINFEKL and labeled with $CFSE^{low}$ or left unpulsed and labeled with $CFSE^{high}$. After incubation for four hours frequencies of $CFSE^{high}$ and $CFSE^{low}$ cells was assess by FACS and specific lysis calculated. Columns represent mean target cell lysis, relative to the unstimulated control. Error bars show SEM. Data are pooled from n=5-13 in at least 5 independent experiments. (G) In vitro coculture assay was set up as in (F). Shown are representative histogram plots gated on CFSE labeled target cells. Low CFSE MFI

*indicate fraction of SIINFEKL pulsed target cells, High CFSE MFI represents fraction of unpulsed target cells. % killing was calculated as in (F). Statistical significance was determined by one way ANOVA for multiple comparisons with * p < 0.05; ** p < 0.01, *** p < 0.001; **** p < 0.0001.*

Various in vivo studies have demonstrated CD8α+ DCs to be the main DC subset with the ability to cross-prime CD8 T cells [50], [56]. And Hochheiser et al found 3pRNA to primarily stimulate CD8α+, but not CD8α- DCs in vivo [57]. However in vitro GMCSF-derived DCs do not contain DCs which phenotypically resemble the splenic CD8α+ DC subset [58]. We therefore attempted to reproduce the coculture experiments described above with splenic DCs, of which a minority (around 20-25% on average) expresses CD8α (Fig. 3A). Splenic DCs stimulated with 3pRNA in the presence of increasing OVA concentrations potently activated OT-I cells to release IFN-γ (Fig. 8A). The differentiation of naive OT-I cells into IFN-γ secreting CD8 effector T cells was peptide specific, as cytokine release was abrogated when OT-I cells and DCs were cocultured in the absence of OVA (Fig. 8B, middle part of figure). There was no direct effect of OVA or adjuvants on OT-I cells, as indicated by the absence of IFN-γ secretion in cultures without DCs (Fig. 8B, right part of figure).

In contrast to IFN-γ secretion, there was no adjuvant effect of 3pRNA or CpG on OT-I proliferation at any tested OVA concentration (1 - 2.2 - 6.7 µg/ml) (Fig. 8C). At a concentration of 6.7 µg/ml, OVA already stimulated 85.5% of CD8 T cells to proliferate, the addition of 3pRNA or CpG did only marginally enhance proliferation by 1.8 (3pRNA) to 5.8 (CpG) percentage points (Fig. 8C). Cross-presentation of OVA-peptide and costimulation of OT-I cells by DCs only slightly contributed to the activation of OT-I cells, the majority of T cell activation was attributable to direct effects of OVA on OT-I cells: The percentage of proliferating T cells decreased by only around 10 percentage points upon the omission of DCs in the culture, but coculture of DCs and OT-I cells in the absence of OVA almost abrogated OT-I proliferation (Fig. 8D).

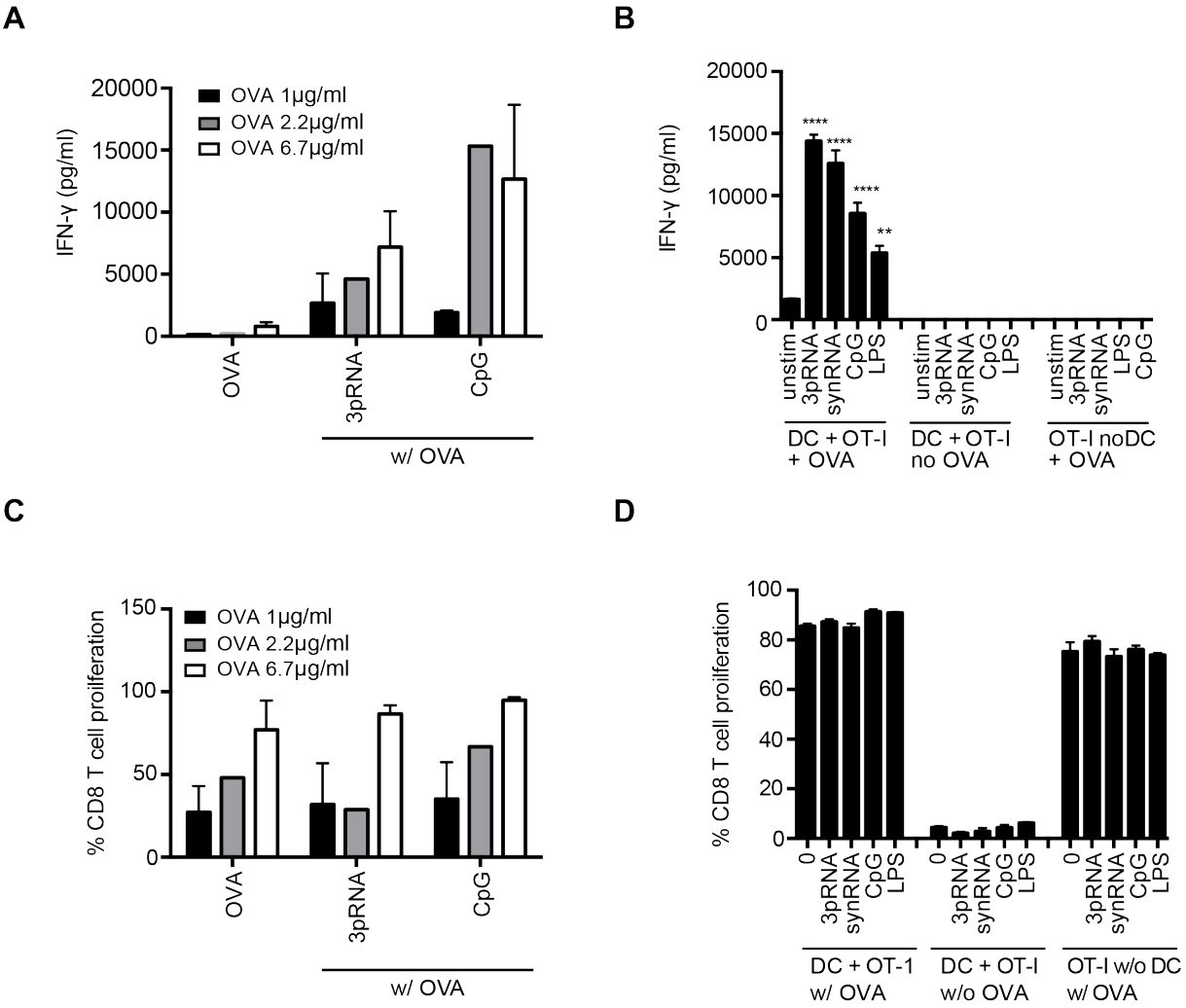

Figure 8: RIG-I activation in splenic DCs efficiently cross-primes OT-I cells.

*Splenic DCs from wild-type C57BL/6 mice were incubated with or without OVA and indicated adjuvant vs medium (as unstimulated control "0") for 1 day. Samples were then cocultured with CFSE labeled OT-I cells for 2-3 days, then samples were analyzed for proliferation with FACS and for IFN- γ secretion by ELISA. (A and C) OVA Titration. SPL DCs were stimulated as described above, but OVA was titrated from 1 -6.7 µg/ml to show induction of proliferation with high OVA doses, but inability to induce IFN-γ by OVA alone. Columns show n=1 for OVA 2.2 or mean of n=2(OVA 1) or n=4 (OVA6.7) with SEM. (B and D) Coculture assay was set up as above. 3 groups were stimulated as above with adjuvant and OVA 6.7 µg/ml, with one group lacking DCs (right part of graph), one group lacking OVA (middle) and one group consisting of DC+OVA+OT-I (left). After 3 days of coculture IFN- γ was analyzed by ELISA and proliferation by CFSE dilution seen with FACS. Columns show mean of technical triplicates, representative for n=2 in 2 independent experiments. Error bars indicate SEM. Statistical significance was determined by one way ANOVA (comparison OVA vs OVA+adjuvant), * p < 0.05, ** p<0.01, *** p<0.001, **** p<0.0001.*

Taken together, our data show that 3pRNA stimulated BMDCs are capable to induce potent CD8 T cell responses in vitro. OT-I cells proliferate, release considerable amounts of IFN-γ and kill target cells in a peptide-specific manner. The induction of IFN-γ secretion in OT-I cultures with GMCSF DCs could be reproduced with splenic DCs and thus confirms the validity of our assay.

5.2.2. Cross-priming of CD8 T cells via RIG-I requires MAVS and IFNaR signaling, but is independent of CARD9

Next we analyzed the contributions of downstream RIG-I pathways in DCs for the induction of CD8 T cell proliferation and differentiation. In the presence of OVA, WT or MAVS deficient BMDCs were stimulated overnight with 3pRNA or the indicated controls and subsequently incubated with OT-I CD8 T cells for 2-3 days in vitro. OT-I proliferation was again assessed by analyzing CFSE dilution with flow cytometry. OT-I differentiation into CTL was determined by IFN-γ production (FACS intracellular stain) or secretion (ELISA).

We already showed that the presence of MAVS is necessary for 3pRNA induced maturation of BMDCs (Fig. 4 and [13]). CD8 T cells require the 3 signals, a mature and licensed DC provides (peptide-MHC-I, costimulatory molecules, pro-inflammatory cytokines) for clonal expansion and differentiation into effector cells [21]–[23]. In line with this we show that MAVS deficient BMDCs are not competent to induce significant OT-I proliferation (Fig. 9A) or IFN-γ secretion (Fig. 9B).

The capacity to induce OT-I proliferation was unchanged with the MAVS-independent PRR ligands CpG and LPS (Fig. 9A). As IFN-γ production and secretion by OT-I cells was decreased if they were cocultured with BMDCs that were pretreated with IFNaR blocking antibody, but preserved in coculture experiments with CARD9 deficient BMDCs, IFN-I seems to play a crucial role in DC maturation (Fig. 5) and subsequent CD8 T cell activation (Fig. 9 C, D, E).

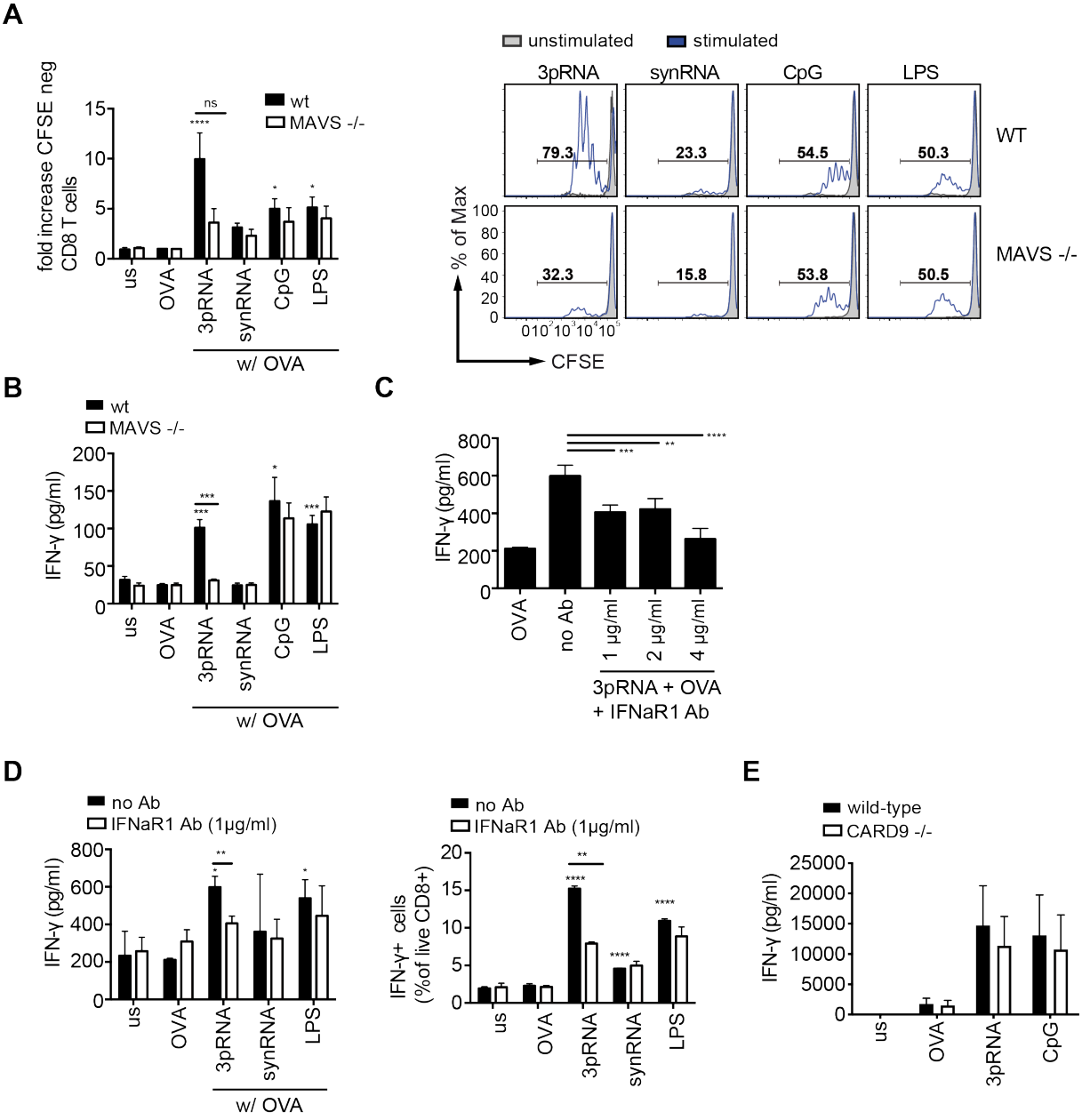

Figure 9: RIG-I induced in vitro cross-priming of OT-I cells depends on MAVS and type I interferon signaling.

(A) Left: wild-type (black columns) or MAVS deficient (white columns) BMDCs were incubated with OVA with or without adjuvant for 1 day, then cocultured with CFSE labeled OT-I cells for 3 days. OT-I proliferation was measured as the percentage of "CFSE negative" cells (undergone at least 1 cell division) and normalized to unstimulated control sample. Columns show mean fold increase of proliferated OT-I cells, pooled from n=6 in at least 3 independent experiments. Error bars indicate SEM. Right: representative histogram plots show percentages of CFSE negative OT-I cells from cocultures with wild-type or MAVS deficient BMDCs and stimulated as indicated above the plots. (B) Columns show mean amount of IFN- γ (with SEM as error bars) in the supernatant of BMDC/OT-I cocultures. BMDCs were generated from wild-type or MAVS deficient mice. Coculture with OT-I was for 2 days. Data was pooled from n=6 per genotype in 4 independent experiments. (C) Data shows mean IFN- γ secretion into the supernatant of wild-type BMDC/OT-I cell cocultures and stimulation with OVA ± 3pRNA. DCs were additionally incubated with titrating doses of a monoclonal IFNaR1 blocking antibody (1 – 4 µg/ml). Graph depicts n=1. (D) Coculture was set up with wild-type BMDCs and OT-I cells in the presence of OVA and indicated stimuli. White columns show mean IFN- γ in the presence of IFNaR blocking antibody (1 µg/ml), black columns show control samples. Error bars indicate SEM. Left graph shows IFN- γ secretion by ELISA (representative of n=3 in 3 independent experiments, mean of technical triplicates), right graph percentage of intracellular IFN- γ as determined by flow cytometry (pooled data of n=2 in 2 independent experiments). (E) IFN-γ secretion after coculture of wild-type (black columns) or CARD9 deficient (white columns) BMDCs together with OT-I cells after stimulation with indicated stimuli. Data pooled from n=5 in 4 independent experiments.

*Statistical significance was determined by one way ANOVA for multiple comparisons and student t-tests for comparison of 2 groups. p < 0.5; **, p < 0.1, ***, p < 0.01; ****, p < 0.001; ns, not significant*

5.3. Analysis of RIG-I mediated cross-priming of CD8 T cells in vivo

5.3.1. 3pRNA treatment enhances vaccination induced CTL expansion

After having shown that RIG-I activation enhances BMDC maturation and subsequent CD8 T cell priming in vitro, our goal was to establish an in vivo model to detect antigen specific CD8 T cell responses, which are ultimately important for the generation of an effective antitumor immune response. Therefore, we adoptively transferred CFSE labeled OT-I splenocytes I.V. into wild-type C57BL/6 mice and immunized mice one day later I.V. with OVA with or without concomitant 3pRNA or control PRR ligands as adjuvant. Three days after vaccination, expansion, proliferation and the ability to produce IFN-γ of the transferred cells was assessed. Using MHC-I/$OVA_{257-264}$ (SIINFEKL) tetramers we were able to demonstrate that the population of OVA specific CD8 T cells in the spleen had increased by more than 10 fold (from 1% to about 11% of all live CD8 T cells) in mice treated with 3pRNA compared to OVA alone (Fig. 10A). Furthermore, 3pRNA induced proliferation of antigen specific T cells, as indicated by CFSE dilution (Fig. 10B). After in vitro re-stimulation of splenocytes with PMA/Ionomycin, we were also able to detect significantly more IFN-γ producing CD8 T cells in mice treated with 3pRNA + OVA (around 10%) compared to immunization with OVA alone (< 1%) (Fig. 10C). CTL expansion and effector function after immunization with OVA is therefore significantly augmented by 3pRNA induced RIG-I activation (Fig. 10).

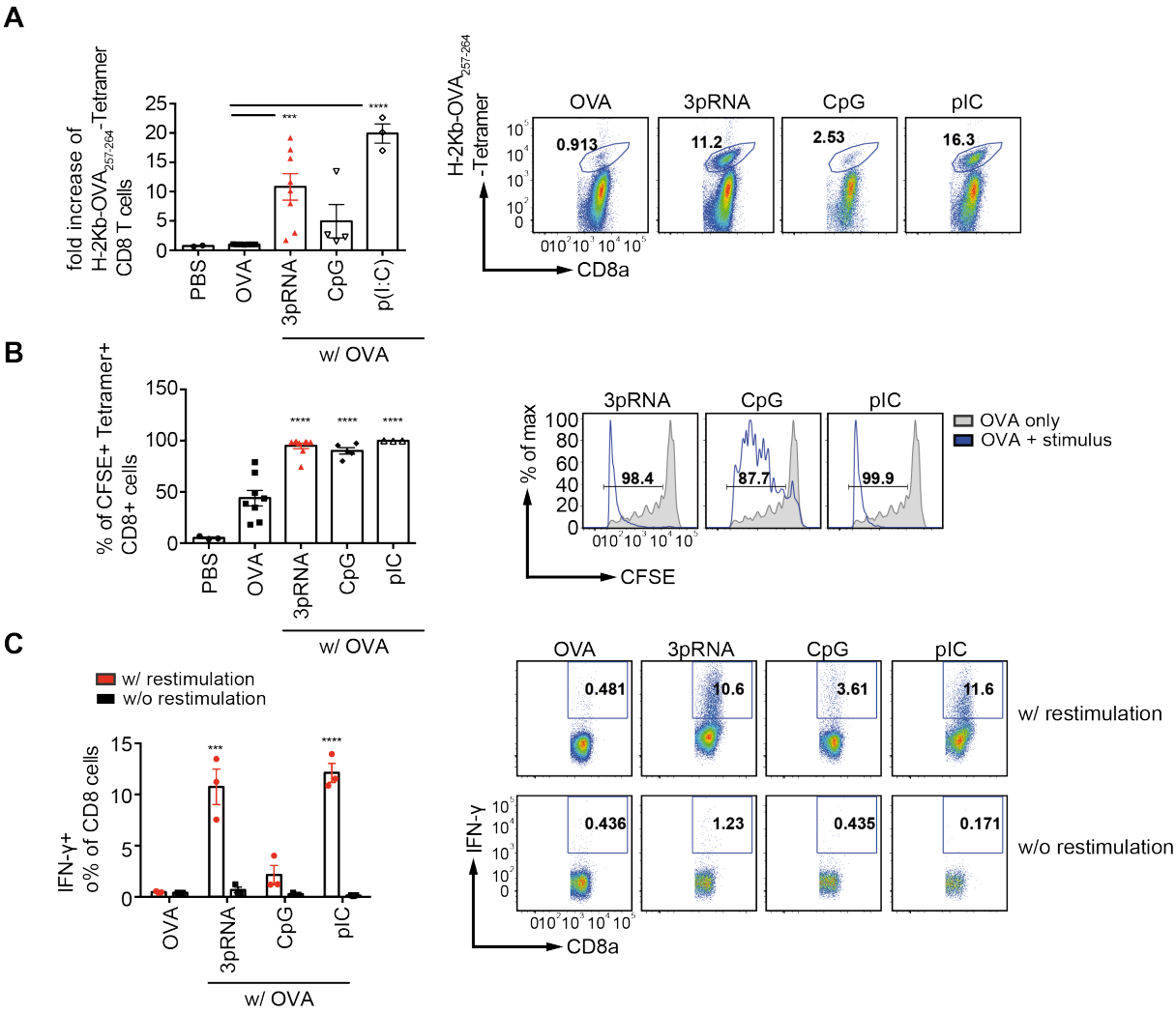

Figure 10: RIG-I activation enhances proliferation and cytokine secretion of adoptively transferred OT-I cells after vaccination with OVA.

*(A) Left: column plot shows fold increase (normalized to PBS control) of frequency of H2kb-SIINFEKL-Tetramer⁺ cells detected in the spleen of recipient wild-type C57Bl/6 mice. Mice were vaccinated with OVA ± indicated adjuvants one day and analyzed four days after adoptive transfer of CFSE labeled OT-I. Right: representative flow cytometry plots show percentage of splenic CD8 T cells binding to H2Kb-OVA257-264-tetramers. (B) Left: OT-I proliferation in spleens of recipient mice was assessed by analyzing the frequency of CFSE^{low} (at least one cell division) among all H2Kb-OVA257-264-tetramer and CFSE positive CD8 T cells. Mice were vaccinated with OVA and received adjuvants therapy as in (A) Right: histogram plots show CFSE signal in H2Kb-OVA257-264-tetramer positive CD8 T cells in the spleens of recipient mice. Grey histogram represents OVA only control. Blue graph represents samples stimulated with OVA+adjuvant. (C) Splenocytes isolated from vaccinated recipient mice were restimulated with OVA in vitro for 1 day, then analyzed for intracellular I IFN- γ production by flow cytometry. All mice were vaccinated with OVA and treated with adjuvants as indicated. Representative flow plots (right) indicate fraction of IFN- γ positive CD8 T cells in the spleens of treated recipient mice. Columns in (A-C) show mean values ± SEM with each data point representing one individual mouse. Data was pooled from 2-6 (A), 3-6 (B) and 1 independent experiment(s) respectively. Statistical significance was determined by one way ANOVA to compare OVA with the OVA+adjuvant samples. ***, p < 0.001; ****, p < 0.0001.*

The use of OT-I cells is an artificial model and depending on the OVA concentration T cells may be activated by OVA alone as shown in our in vitro studies (Fig. 6A). Therefore, we established a vaccination model that took advantage of endogenous OVA specific CD8 T cells. C57BL/6 mice were injected S.C. in the hindfoot with OVA with or without 3pRNA or the indicated control PRR ligand. The treatment was

repeated on day 7. After another 5 days the regional LN and spleen were harvested and analyzed. There was a strong regional immune response indicated by increased total cell count in the popliteal LN (Fig. 11A). SIINFEKL specific CD8 T cells expanded more than 3-fold and also secreted IFN-γ (Fig. 11B). To demonstrate peptide specific CD8 T cells as source for the IFN-γ detected by ELISA, whole LN cells were restimulated in vitro with OVA for 72 hours. Only in samples incubated with OVA IFN-γ was detectable (Fig. 11B). This finding was proofed by FACS analysis showing an expansion of IFN-γ^+SIINFEKL-Tetramer$^+$ cells by about 2-fold in regional LN of mice treated with 3pRNA as adjuvant (Fig. 11C). Using this assay we were not able to see an expansion of SIINFEKL specific CD8 T cells in the spleen, despite a robust secretion of IFN-γ in OVA restimulated splenocytes (Fig. 11D).

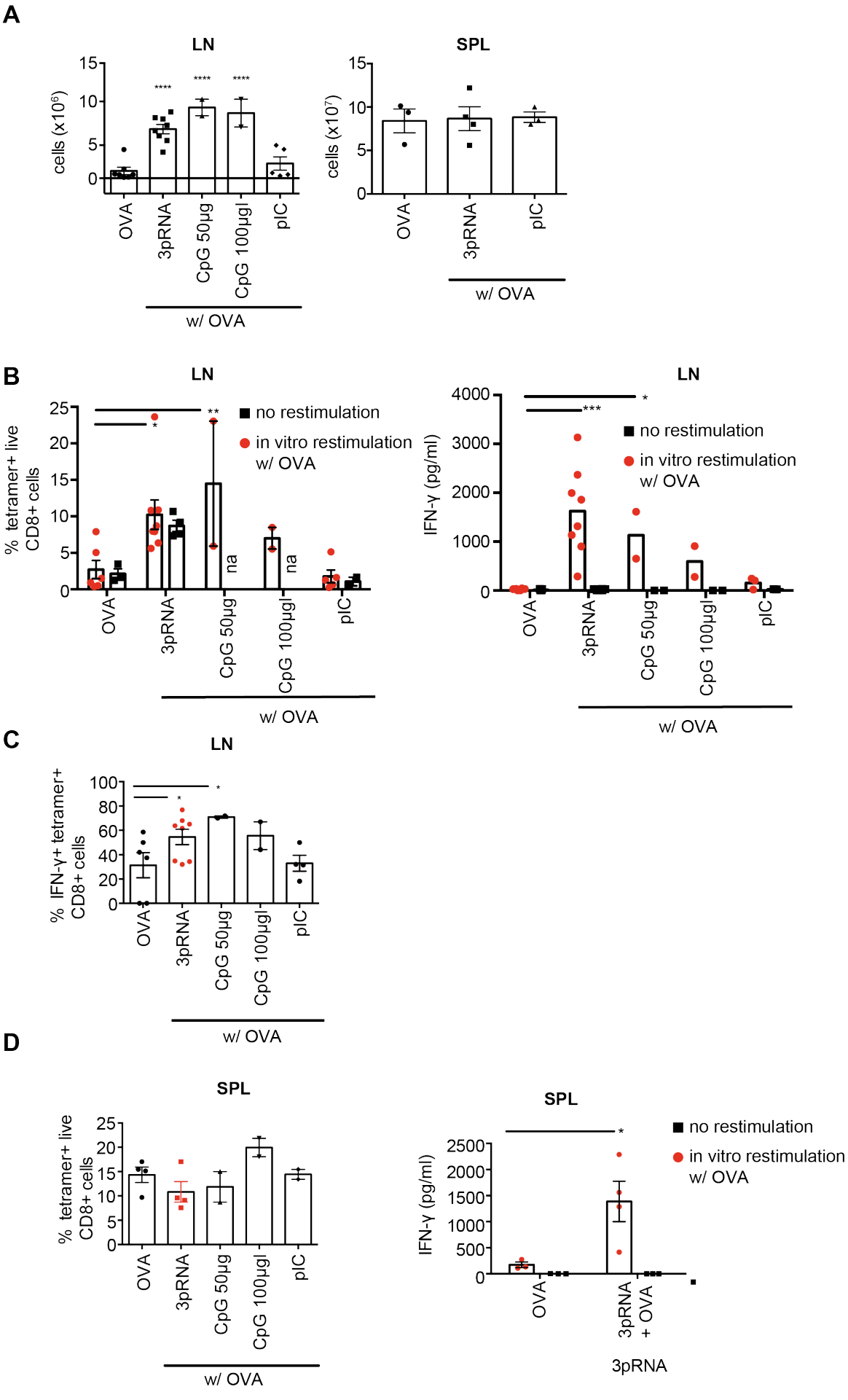
A
LN
SPL
cells (x10⁶)
cells (x10⁷)
OVA
3pRNA
CpG 50µg
CpG 100µgl
pIC
w/ OVA
B
LN
% tetramer+ live CD8+ cells
no restimulation
in vitro restimulation w/ OVA
na
IFN-γ (pg/ml)
C
% IFN-γ+ tetramer+ CD8+ cells
D
SPL
3pRNA + OVA
3pRNA

Figure 11: Regional CTL response after OVA vaccination is enhanced by 3pRNA adjuvants.

*Wild-type recipient mice were vaccinated with OVA ± indicated adjuvant S.C. in the hindfoot. Treatment was applied twice, one week apart and recipient mice were analyzed five days after the second vaccination. (A) Shows mean total cell counts of (left) regional (popliteal) lymph nodes or (right) spleens with error bars indicating SEM. All animals received OVA vaccines and adjuvants (3pRNA 25 μg, CpG or p(I:C) 25 μg) as indicated. (B) Whole LN cells were (red dots) or were not (black square) restimulated with OVA in vitro for 3 days and expansion of tetramer positive cells (left graph) and IFN- γ secretion (right graph) analyzed by FACS and ELISA respectively. (C) whole LN cells were restimulated with OVA in vitro as above, then analyzed for intracellular IFN-γ by FACS. (D) Left graph: Whole splenocytes were restimulated with OVA in vitro then analyzed for SIINFEKL-Tetramer⁺cells by FACS. Right graph: 50% of the samples were restimulated with OVA and IFN-γ secretion was analyzed by ELISA. Columns in (A-D) indicate mean values ± SEM with each data point representing one individual mouse. Data was pooled from 2 independent experiments for A, B, C and is from one experiment for D. Statistical significance was determined by one way ANOVA for comparison of OVA with OVA+adjuvants. * p < 0.05; ** p < 0.01; *** p < 0.001, **** p<0.0001.*

Our laboratory had shown earlier that CD4 T cells upregulate CD69, an early activation marker, in vivo following 3pRNA administration [41]. The assay we used here failed to show induction of IFN-γ production in CD4 T cells in the regional LN (Fig. 12A) and the spleen (Fig. 12B) following S.C. administration of 3pRNA and OVA and in vitro restimulation with OVA. Also screening for a cytokine profile favoring certain CD4 subsets failed to demonstrate skewing of a RIG-I induced CD4 T cell response: IL-17, IL-2, IL-4 and IL-10 were undetectable in LN cells after in vitro re-stimulation with OVA (data not shown).

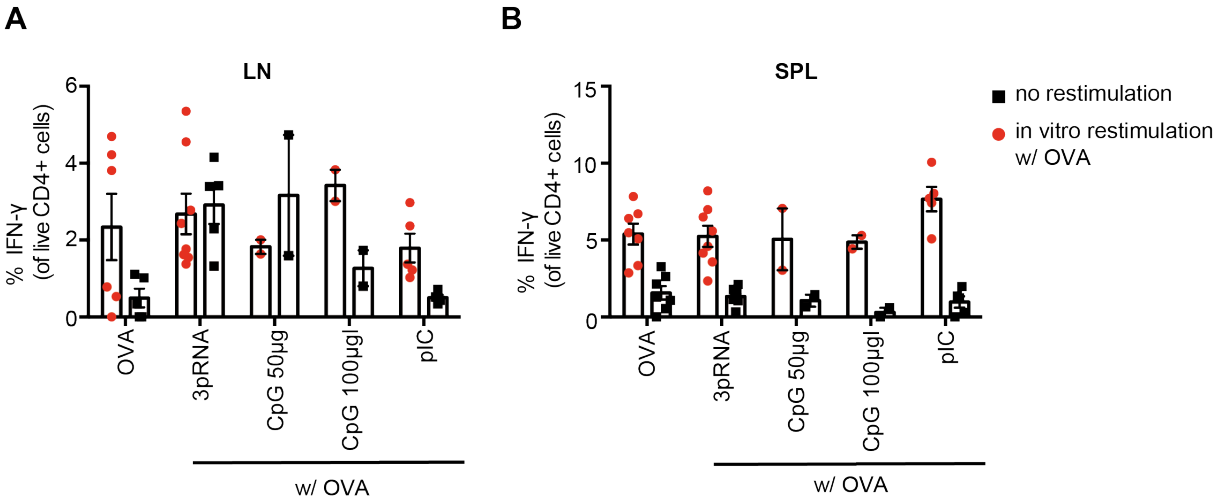

Figure 12: 3pRNA does not induce IFN-γ production in CD4 T cells in regional LN or spleen after vaccination with OVA.

Wild-type C57Bl/6 mice were vaccinated with OVA 3μg ± indicated adjuvants twice, one week apart. Animals were analyzed five days after the second vaccination. Vaccination was performed via injection into the hindfoot. Column charts show intracellular % of IFN-γ positive cells among live CD4⁺ cells in the regional LN (A) or in the spleen (B) with or without restimulation with OVA in vitro for 3 days. Data points indicate individual mice, columns show mean of n=2-8 in 2 independent experiments. Error bars indicate SEM.

Overall, using OVA as a model antigen, we were able to show that RIG-I ligation can be used as an effective adjuvant to boost the induction of an antigen-specific CD8 T cell response after OVA vaccination.

5.3.2. RIG-I activation induces CTL mediated lysis of target cells in vivo

In our previous experiments we have established that 3pRNA mediated RIG-I activation enhances vaccination with a model antigen by selective expansion of antigen-specific IFN-γ producing CD8 T cells. Next we wanted to determine whether expanded CTL also have antigen specific cytolytic activity. For this we immunized wild-type C57BL/6 mice with PBS, OVA ± 3pRNA or the indicated control I.V. (Fig. 13C, D) or S.C. in the hindfoot (Fig. 13A, B). 6 days later a 1:1 mix of target (SIINFEKL pulsed, $CFSE^{low}$) and non-target cells (no peptide, $CFSE^{high}$) was injected into the tail vein. One day later, spleens of recipient mice were analyzed for the presence of transferred target cells. To obtain “target cells”, whole splenocytes of syngeneic donor mice were tagged with SIINFEKL, the immunogenic OVA peptide, followed by staining with a low concentration of CFSE ($CFSE^{low}$). Non-target cells were splenocytes not tagged with SIINFEKL and stained with a high concentration of CFSE ($CFSE^{high}$).

Using 30 µg OVA (in contrast to 3 µg in Fig. 11), we were able to elicit an expansion of SIINFEKL specific CD8 T cells in the spleen following S.C. vaccination with 3pRNA + OVA (Fig. 13B). These cells acquired effector function and eliminated 70-80% of the SIINFEKL pulsed target cells, but not the un-pulsed control cells (Fig. 13A). Administration of antigen and 3pRNA I.V. resulted in slightly higher SIINFEKL specific CD8 T cell frequencies (Fig. 13C), but efficiency in target cell elimination was similar compared to the S.C. route (Fig. 13D).

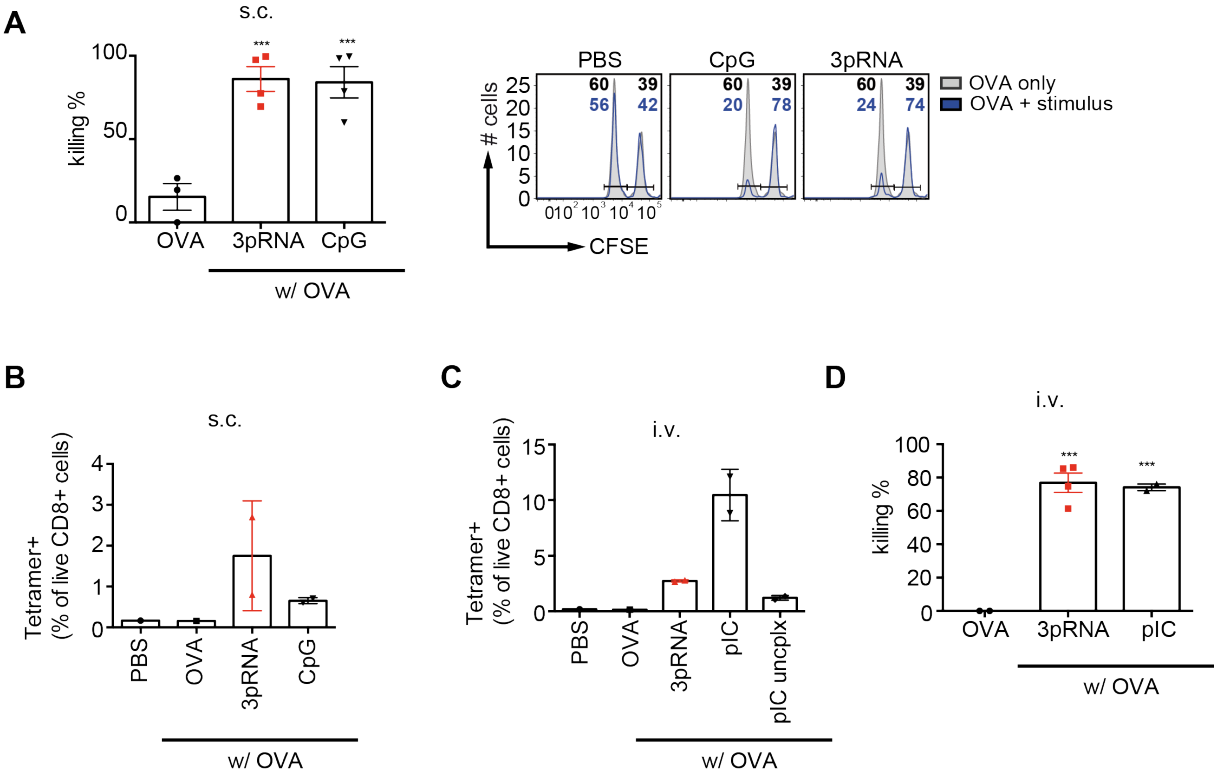

Figure 13: RIG-I activation enhances lysis of target-cells in vivo after vaccination with target antigen.

*Wild-type C57BL/6 mice were vaccinated with PBS, OVA or OVA+adjuvant. Vaccination was performed by either S.C. injection in the hindfoot (A, B) or I.V. injection into the tail vein (C, D). 6 days after vaccination, target cells were adoptively transferred by I.V. injection into the tail vein. Target cells represent splenocytes of wild-type C57BL/6 mice, which were either tagged in vitro with SIINFEKL and labeled with low dose of CFSE ($CFSE^{low}$), or left untreated but labeled with high dose of CFSE ($CFSE^{high}$). Target cells were mixed and transferred at a ratio of 1. After 24 hours, target cell frequencies in the spleen were analyzed. Killing was calculated using the formula 100-(sample $CFSE^{low}$/sample $CFSE^{high}$)/control $CFSE^{low}$/control $CFSE^{high}$) with PBS being the control. (A) Columns show mean specific lysis, of n=3-4 in 2 independent experiments after S.C. vaccination with OVA±CpG or 3pRNA. Flow cytometry plots show fractions of $CFSE^{low}$ and $CFSE^{high}$ target cells in spleens of mice with S.C vaccination as in A. Plots are representative of pooled data in A. Grey histograms represent cells from PBS only control mice, blue histograms those from OVA±CpG or 3pRNA treated mice. (B) shows the mean fraction of splenic SIINFEKL-specific CD8 T cells after S.C. vaccination, data points indicate individual mice in 1 experiment. OVA specificity was determined by H2Kb-$OVA_{257-264}$-tetramer flow cytometry staining. (D) Columns indicate mean peptide specific lysis of n=2-4 in 2 independent experiments or (C) mean percentage of H2Kb-$OVA_{257-264}$-tetramer positive CD8 T cells of n=1-2 in 1 experiment in spleens of mice which received I.V. vaccination with PBS or OVA± indicated adjuvants. All error bars indicate SEM. Statistical significance was determined by one way ANOVA for comparison of OVA with OVA+adjuvant. *** p < 0.001.*

Taken together we show that RIG-I activation by 3pRNA enhanced the expansion of vaccination induced CD8 T cells. The strong adaptive immune answer was antigen specific and led to lysis of adoptively transferred target cells.

5.3.3. RIG-I mediated CTL induction is MAVS dependent in vivo

In in vitro coculture experiments we already established an important role of MAVS for the maturation of DCs following RIG-I ligation and subsequent priming of CD8 T cells (Fig. 4, 9). Next, we asked if the RIG-I – MAVS axis is also necessary for the generation of antigen-specific CTLs in vivo. We transferred CFSE labeled OT-I cells in C57BL/6

and MAVS deficient mice. The next day mice were injected I.V. with OVA with or without 3pRNA or CpG. The frequencies of transferred OT-I cells in the spleens of experimental animals were analyzed 3 days later. The population of tetramer positive cells increased from around 1% in the OVA only control to 7 and 14% in the two WT mice treated with 3pRNA. This effect was markedly reduced in MAVS deficient recipient mice (Fig. 14A). The reduced adaptive immune response after RIG-I stimulation in MAVS deficient mice was accompanied by decreased production of IFN-γ by adoptively transferred OT-I cells as determined by FACS (Fig. 14B, 40 times more IFN- γ positive cells among CFSE+CD8+ cells in 3pRNA+OVA treated mice compared to OVA and reduction by 50% in MAVS deficient mice). Also IFN-γ and TNF-alpha secretion by endogenous cells in regional LN following S.C. injection of OVA + 3pRNA was impaired in MAVS deficient mice (Fig. 14 C). This confirms that 3pRNA mediated expansion of peptide specific CD8 T cells and their differentiation into IFN-γ producing CTLs in vivo is dependent on MAVS expression.

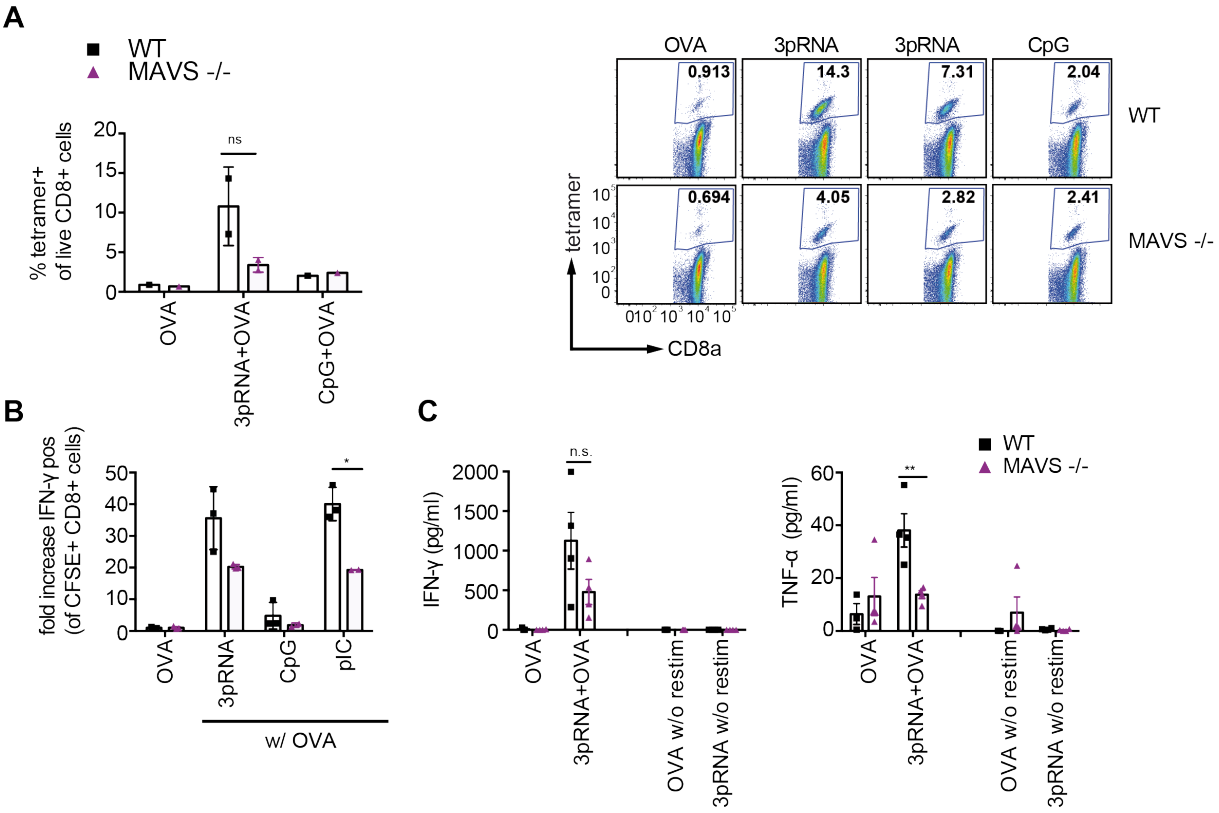

Figure 14: In vivo expansion and cytokine secretion of antigen specific CTL after vaccination with OVA+3pRNA is MAVS dependent.

(A) OT-I cells were injected I.V. into wild-type C57Bl/6 (black squares) or MAVS deficient mice (purple triangle) followed by I.V. treatment with either OVA alone or OVA+adjuvant as indicated (OVA 3μg, 3pRNA 15μg, CpG 19μg). Left chart: columns show mean percentages of OVA-specific CD8 T cells as determined by H2Kb-OVA$_{257-264}$-tetramer staining in the spleens of mice with indicated treatment regiments. Right flow cytometry plots are representative of frequencies of

SIINFEKL-tetramer+ CD8 T cells and show H2Kb-OVA257-264-tetramer+ CD8+ cells among total live splenocytes. Upper row shows data from wild-type mice, lower row from MAVS deficient animals. (B) OT-I transfer and I.V. vaccination as in A, however with OVA 3μg, 3pRNA 25μg, CpG 15μg. Samples were restimulated in vitro with OVA for 1 day. Columns show mean fold increase of IFN-γ positive cells among all live CD8+ CFSE+ cells relative to the negative control OVA. (C) IFN-γ production by endogenous cells: WT (black square) and MAVS deficient mice (purple triangle) were vaccinated S.C. in the hindfoot with OVA 3μg or OVA+ 3pRNA 25μg twice 7 days apart and the regional LN was analyzed 4 days later. Whole LN cells were restimulated in vitro with OVA or medium (control) for 3 days then supernatant was analyzed with CBA for IFN-γ (left) or TNFα secretion (right). Columns indicate mean of 2-3 mice in 1 experiment.

*Error bars indicating SEM. Statistical significance was determined by students t-tests for comparison WT/MAVS with * p < 0.05; ** p < 0.01; ns, not significant.*

5.4. Effects of vaccination with a RIG-I ligand on tumor progression in vivo

In previous experiments we were able to show that 3pRNA induced RIG-I activation in DCs enhances an antigen specific adaptive immune response. Next, we examined if the 3pRNA + OVA induced CTL response would protect vaccinated WT mice from progression of an OVA expressing tumor if challenged after vaccination. First, we monitored progression of OVA expressing B16 murine melanoma cells (B16-OVA) that were injected into the flank of naïve C57BL/6 mice, with initial tumor load being 15 000 – 1.5 M cells. Tumor size was measured daily and mice were sacrificed if the tumor ulcerated or exceeded 15mm in diameter (Fig. 15A). For future tumor experiments an initial tumor burden of 450 000 cells was selected. Next, C57BL/6 mice were vaccinated S.C. in the hindfoot with OVA (3 μg) with or without 3pRNA (15 or 25 μg). 14 days later 450 000 B16-OVA cells were injected S.C. in the ipsilateral flank. Fig. 15B depicts tumor sizes in experimental animals over time. Except for day 12 differences between OVA and OVA + 3pRNA were not statistically significant, however there was a vague trend of delayed tumor progression in 3pRNA vaccinated mice compared to peptide alone.

In an attempt to enhance the prophylactic anti-tumor effect in a new tumor model, mice were treated twice, 14 days apart with OVA (3 μg) and jetPEI as negative control or OVA + 3pRNA (25 μg). 5 days later mice were challenged with S.C. injection of B16-OVA cells as described above. Fig. 15C shows similar results as in the previous un-boosted vaccination model, with possibly slightly delayed tumor progression, but no clear differences.

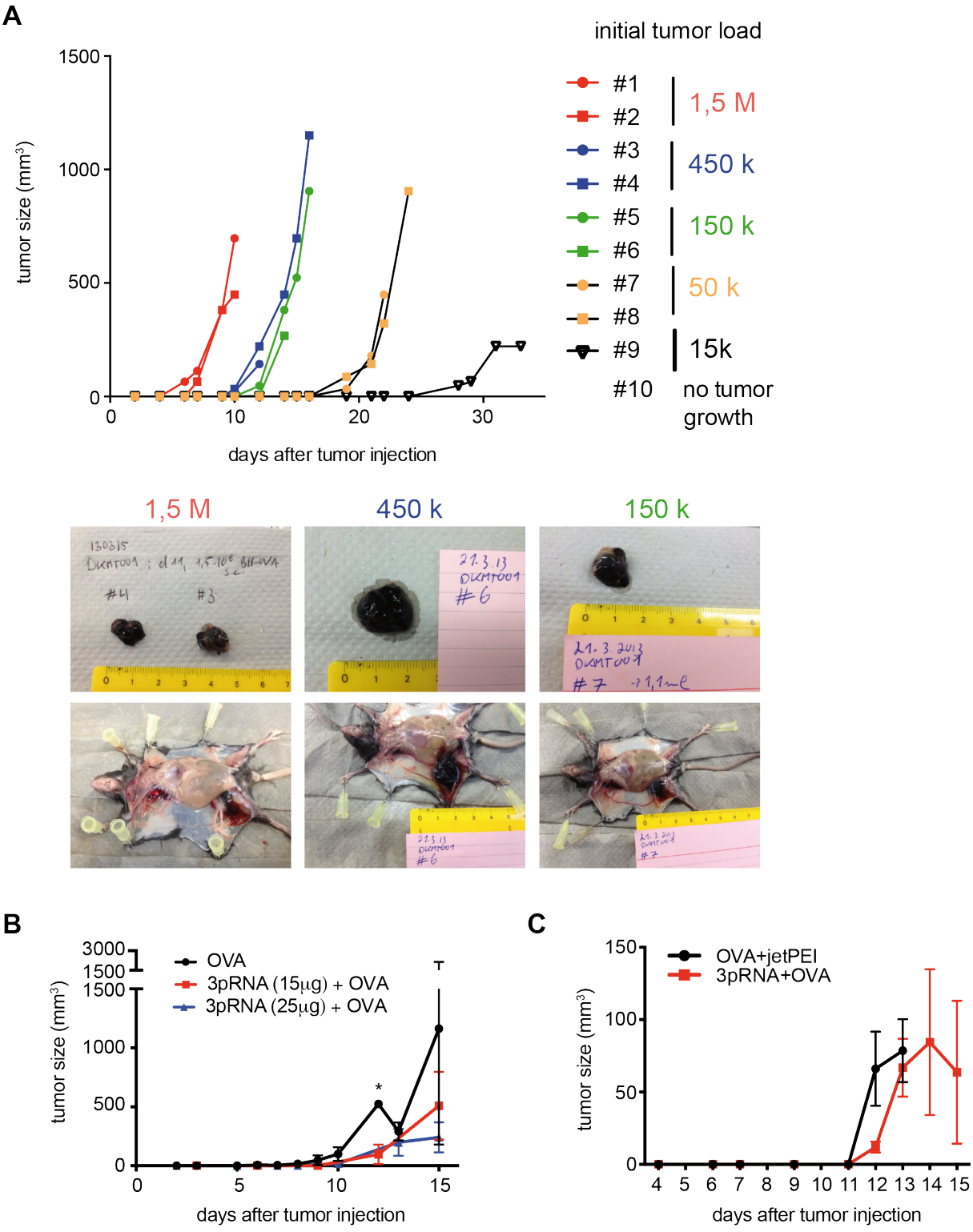

Figure 15: RIG-I vaccination may lead to improved outcome in B16 tumor model.

(A) Different numbers of B16-OVA tumor cells were subcutaneously injected into the flank of wild-type C57BL/6 mice. Tumor growth was measured daily and mice were sacrificed if the tumor ulcerated or exceeded 15mm. Each symbol indicates one mouse, each color the same amount of injected B16-OVA cells. Photographs are representative of mice and tumors on day of analysis. (B) Recipient mice were vaccinated S.C. in the hindfoot with OVA 3µg alone (black) or additionally received 3pRNA as adjuvants (15 or 25 µg/ml). 14 days later 450 000 B16-OVA cells were injected S.C. in the ipsilateral flank and tumor growth was monitored. Data is pooled form n=2 – 6 in 2 independent experiments. Mice were sacrificed on day 12 (OVA), 13 (3pRNA 25, 3x OVA mice) and 15 (remaining animals). (C) C57BL/6 mice were vaccinated S.C. in the hindfoot twice, 14 days apart. Vaccines were OVA 3µg + jetPEI or OVA+3pRNA 25µg. On day 19 450 000 B16-OVA cells were injected S.C. in the ipsilateral flank and tumor growth monitored. Data was pooled from n=6 per group in 1 experiment.

*Error bars indicating SEM. Statistical significance was determined by students t-tests for comparison OVA/OVA+3pRNA with * $p < 0.05$.*

6. Discussion and Summary

6.1. RIG-I induced cross-priming of CTL in vitro

Adaptive immune responses targeting infected and dysplastic cells are pivotal for host health and are the cornerstone of modern cancer immunotherapies. Expansion of antigen specific CD8 lymphocytes requires additional innate help and includes processing of exogenous proteins and cross-presentation via MHC-I. Central mediators bridging innate and adaptive immunity are DCs and activation of their PRR effectively supports antigen specific immune responses. The viral sensor RIG-I stands out from other PRR family members as it is ubiquitously expressed in all cell types including cancerous cells, has a well described ligand and RIG-I activation has been associated with favorable outcomes in preclinical tumor models. The exact mechanisms and involved pathways are not completely understood so far but a combination of tumor intrinsic RIG-I activation and boosting adaptive anti-tumor immunity is likely [41], [59], [60].

The in vitro experiments in this thesis are based on the generation of GMCSF induced BMDC. There are two central classes of dendritic cells: conventional dendritic cells (cDC) and plasmacytoid dendritic cells (pDCs) [61]. cDCs have been described to be superior to pDCs with regard to processing and presentation of antigens, upregulation of costimulatory molecules and thus are more efficient in priming naive T cells whereas pDCs are more potent in secreting IFN-I in response to viral infections [61]. For in vitro studies we weighed two options of DC cultures: bone marrow differentiation with (1) GMCSF, that generates cells resembling cDCs [58] and (2) Flt3 ligand that allows cells to differentiate in a heterogenous population of cDC- and pDC-like cells [61], [62]. As the primary goal of this study is to analyze the RIG-I mediated cross-priming of CD8 T cells, we chose the aforementioned method, prioritized GMCSF DC's ability to potently prime T cells.

Our experiments showed that RIG-I ligation in BMDCs results in their maturation in vitro including the expression of costimulatory molecules, secretion of proinflammatory cytokines (IL-6, IL-12p40) and secretion of large amounts of IFN-α, a cytokine known to be central in the immune defense against viruses [43] and dysplastic cells [63] (Fig. 2). 3pRNA mediated BMDC maturation was independent of ASC, but almost abrogated in MAVS deficient BMDCs (Fig. 4). This indicates a pivotal role of either NFκB activation or the IRF3/IFN-I axis as both pathways rely on signal transduction by MAVS [13]. Upregulation of costimulatory molecules following RIG ligation was drastically decreased in IFNaR deficient BMDCs, but independent of the signaling protein CARD9, suggesting that 3pRNA induces BMDC maturation by IFN-I in an autocrine feed-forward loop (Fig. 5). This could be confirmed in later published work showing strict dependence on MAVS and IFN-I expression in DCs to control West Nile Virus (WNV) infection, a virus that is known to be recognized by RIG-I: Myeloid specific deletion of MAVS and IFNaR resulted in cytokine storm, sepsis and endorgan damage through unrestricted viral replication [64]. However, there was still a slight residual upregulation of costimulatory molecules, MHC-I and -II in IFNaR deficient BMDCs indicating that IFN-I independent 3pRNA mediated effects also play a role in DC maturation (Fig. 5). This is in contrast to findings from Honda et al who showed that p(I:C) mediated DC activation is abolished in IFNaR deficient DCs.[65]. This can likely be attributed to off-target effects of our in vitro transcribed 3pRNA.

To monitor cross-presentation and CTL activation we took advantage of the well-established TCR transgenic OT-I mouse line. CD8 T cells bearing the transgenic TCR specifically recognize the peptide SIINFEKL ($OVA_{257-264}$) which enabled us to monitor antigen-specific CD8 T cell responses to a commercially available peptide (adapted from [48]). As expected, CTL proliferation and IFN-γ production were dependent on MAVS expression (but not CARD9) in BMDCs and could also be abrogated by antibody mediated IFNaR1 blockage (Fig. 9).

According to the “three-signal model” of CTL instruction, naïve CD8 T cells require (i) recognition of antigen/MHC complexes, (ii) activation through costimulatory molecules and (iii) uptake of proinflammatory cytokines such as IL-12 or IFN-I [23]. Our data in conjunction with previously published studies allow the hypothesis that in RIG-I

mediated cross-priming of CTLs all 3 signals heavily rely on the secretion of IFN-I by DCs:

IFN-I has been shown to induce maturation of human [66] as well as murine BMDCs [65]. This is in line with our findings of severely decreased upregulation of CD80 and -86 (Fig. 5) as well as impaired cross-presentation of exogenous OVA on MHC-I (data not shown, [67]). Despite the importance of IFN-I for CD8 T cell expansion and differentiation into memory cells [68], Hochheiser et al showed that RIG-I mediated CTL responses mostly depend on IFN-I effects on DCs [57].

6.2. RIG-I induced cross-priming of CTL in vivo

The adoptive transfer of OT-I cells is a reliable model with a known population of naïve OVA specific CD8 T cells and allows analysis of in vivo cross-priming. We were able to demonstrate expansion of OT-I cells and differentiation into IFN-γ producing CTLs following I.V. administration of 3pRNA and OVA (Fig.10). Despite its convenience it is an artificial model and as shown in our in vitro studies, high concentrations of OVA can directly stimulate OT-I cells to proliferate (Fig. 8D), therefore we confirmed our findings with endogenous CD8 T cells. Subcutaneous vaccination of WT mice with additional boost vaccination induced expansion and IFN-γ secretion by endogenous OVA specific CD8 T cells in the regional LN and at higher OVA doses (30μg instead of 3μg) also in the spleen (Fig. 11 and 13). Those expanding CD8 T cells were functional CTLs, capable of peptide specific target cell elimination (Fig. 13). When MAVS deficient mice were treated with 3pRNA, CTL expansion and IFN-γ secretion showed a trend towards MAVS dependence although statistical significance was not reached, likely due to low number of experimental animals (Fig. 14).

In this work we focused on RIG-I mediated maturation of DCs and subsequent cross-priming of CD8 T cells. Triggering different classes of PRRs in DCs creates a particular cytokine milieu that determines the fate not only of CD8 T cells (anergy vs effector function), but also of naïve CD4 T cells. Little data exists on RIG-I mediated polarization of T helper cells, however Cella and colleagues showed that human pDCs infected with Influenza virus, a known RIG-I stimulus, potently skewed naïve CD4 T cells towards Th1 cells in vitro [69]. In our in vivo vaccination model, we were not able to elicit an expansion of CD4 T cells or their differentiation into IFN-γ producing effector

cells (Fig. 12). Further experiments are necessary to analyze the effect of RIG-I activation in DCs on CD4 T cells.

6.3. RIG-I activation as a treatment modality for cancer

We combined in vitro coculture assays and in vivo vaccination models with genetic ablation of signaling proteins to define a crucial role of the RIG-I – MAVS – IFN-I axis during this process. IFN-I has been shown to play a pivotal role in tumor rejection [63], [70], [71] and cross-priming of CD8 T cells [21], [34]. RIG-I ligation combines the induction of large amounts of IFN-I, cross-priming of CTLs and the induction of immunogenic cell death in transfected tumor cells - all features that render RIG-I ligands interesting candidates for cancer immunotherapy.

In this study we were able to show a vague trend towards delay of tumor progression after prophylactic vaccination with 3pRNA and the model protein OVA (Fig. 15 B, C). In addition to flaws in the experimental design (e.g. low OVA concentration, timing, early dropouts of mice due to tumor ulceration), IFN-I induced upregulation of immunosuppressive factors might have limited the effect [72].

Antibody mediated blockade of immune checkpoints has revolutionized the treatment of many, especially advanced malignancies [27], [28]. However a pre-requisite for the successful use of this approach seems to be a pre-existing anti-neoplastic immune response: The abundance of tumor infiltrating lymphocytes (TIL) have been shown to be a predictor of response to checkpoint inhibition with anti-PD1 therapy (pembrolizumab) in metastatic melanoma in humans [37]. Moreover, the presence of TIL in human colorectal cancer correlates with a more favorable outcome in general [39], [73]. For the spontaneous generation of a “T cell inflamed tumor microenvironment” [74] the pivotal driver seems to be IFN-I secreted by DCs and subsequent priming of tumor-specific CD8 T cells [63], [70], [75]. Common PRR pathways including MyD88, TRIF, TLR4, TLR9 and MAVS have been shown to be dispensable for the induction of IFNy producing CD8 T cells in mice challenged with an immunogenic tumor (B16.SIY). STING KO mice however were not capable to mount a CD8 T cell response after I.V. injection of cancer cells or to control the growth of an adoptively transferred immunogenic cancer cell line. [38]. STING deficient mice

are also more prone to develop colitis associated colorectal cancers [76]. Taken together STING seems to play an important role in the physiologic immune response against immunogenic cancers. However not all malignancies generate a T cell inflamed tumor microenvironment. Based on this knowledge, different strategies are currently emerging to boost antitumor immune responses. One approach is to prime endogenous T cells in vitro with tumor antigens before reinfusion [77], [78]. Chiapinelli et al demonstrated upregulation of nucleic acid sensing pathways in tumors following treatment with chemotherapy (Azacytidine) and subsequent IFN-I dependent tumor sensitization to ICB and apoptosis [79]. This allows the hypothesis that also the direct stimulation of those receptors would increase responses to ICB.

In further experiments in our laboratory we therefore also combined RIG-I mediated priming of CTL with ICB (CTLA-4 blockade): Prophylactic vaccination with OVA and 3pRNA partially protected mice from lung metastasis when challenged with an OVA bearing tumor cell line, an effect that was markedly enhanced when vaccination was combined with anti-CTLA4 [67]. Also in a therapeutic setting combination of 3pRNA and ICB achieved the maximum effect in regards to tumor regression [67]. This is likely due to RIG-I activation in DCs as well as tumor intrinsic RIG-I signaling: tumor intrinsic RIG-I signaling was not only shown to be key to ICB responsiveness, but also induces immunogenic tumor cell death and subsequent cross-priming of CTL and CTL mediated tumor regression [60], [80].

The clinical relevance of these findings is highlighted by a recently published study from Such et al: human melanoma cells derived from patients not responding to ICB treatment have decreased expression of HLA-I allowing the tumor to escape from T cell surveillance which results in lower overall survival in those patients. Treatment with 3pRNA restored HLA-I expression and ICB responsiveness. Interestingly this effect was IFN-I independent (IFNaR KO, STING KO) [81].

Several other groups confirmed the anti-tumor effects of RIG-I activation in preclinical studies and demonstrated the efficiency of different RIG-I agonists and routes of administration.

For any pharmaceutical pharmacokinetic considerations are important. For oligonucleotides in cancer therapy especially the stability of the construct and the delivery to the target cells (in this case the cytoplasm of tumor cells and DCs). A

synthetic RIG-I agonist with stem loop structure described by Linehan et al is thought to have enhanced stability for in vivo applications and has been successfully used in murine models for breast cancer [82], melanoma and colorectal cancer [83]. For our in vivo experiments we used jetPEI, that is known to predominantly accumulate in liver, lungs, spleen and kidney [41]. Though no cell type specific delivery of oligonucleotides is available yet, there is ongoing research for alternate carriers. Wilson et al developed a nanoparticle that complexes oligonucleotides and peptides and thus allows “dual-delivery” of antigen and adjuvant and subsequent enhanced cross-presentation and CD8 T cell activation [84]. These nanoparticles have been shown to be effective in a murine breast cancer model [82]. Interestingly, not only solid tumors seem to be responsive to RIG-I mediated anti-cancer therapy: after I.V. inoculation of green fluorescent protein (GFP) expressing acute myeloid leukemia (AML) cell lines, treatment with 3pRNA not only led to a decreased abundance of tumor cells in peripheral tissues but also to a survival benefit. Noteworthily, the anti-tumor effect seemed to be mediated by CD4 and CD8 T cells as the survival benefit was reversed after treatment with anti-CD4 and anti-CD8 antibodies. As AML cells also upregulated PD1 upon RIG-I induced secretion of IFN-γ, treatment with checkpoint inhibitors boosted therapeutic efficiency [85].

6.4. RIG-I agonists in clinical trials

Encouraging results of preclinical studies using RIG-I agonists in tumor models in combination with evidence that RIG-I expression in human melanoma cells correlates with overall survival and response to ICB, supports a potential benefit of RIG-I agonists in cancer therapy [80].

The synthetic RIG-I ligand SLR20 that showed efficacy in a preclinical breast cancer model was one of the first RIG-I agonists used in a Phase I/II clinical trial. Adult patients with advanced or recurrent solid tumors or lymphomas received intratumoral injections twice per week with escalating doses. Overall MK-4621 administration appeared to be tolerable without causing dose-limiting toxicities (MK-4621-001/RGT100-001, ClinicalTrials.gov, Identifier: NCT03065023, [86])

Another ongoing Phase I clinical trial currently evaluates the same compound in combination with pembrolizumab as a treatment option for recurrent/advanced solid cancers (MK-4621-002, ClinicalTrials.gov, Identifier: NCT03739138)

CureVac developed CV8102 (also termed RNAdjuvant®), a non-specific RIG-I agonist which also triggers TLR7 and TLR8 activation. CV8102, a noncoding ssRNA which contains polyU repeats and is stabilized by a cationic carrier peptide, has been shown to improve the antitumor response in a preclinical syngeneic model using TC-1 tumor cells (a murine model of HPV-induced cervical cancer) through the generation of tumor antigen specific CD8 cytotoxic T cells [87]. A recent Phase 1 trial evaluated the safety and feasibility of intratumoral CV8102 ± pembrolizumab in patients with advanced solid tumors including squamous cell carcinoma of the skin or head/neck, melanoma or adenoid cystic carcinoma. Enrolled patients were treated with up to eight injections over a period of 12 weeks (ClinicalTrials.gov, Identifier: NCT03291002). Anecdotal data of this trail showed promising results including achievement of stable disease in 7/20 patients and complete regression of injected as well as non-injected lesions in 1/20 patients [88].

Improving treatment options and outcomes of cancer patients who developed resistance to standard chemotherapy still represents a major challenge. However, a promising strategy emerged in recent years which is to hijack highly effective immune mechanisms that have originally coevolved to protect us against a plethora of microbial and non-microbial threats and to utilize these immune pathways to turn our immune system against neoplastic cells. In this thesis, we were able to demonstrate that a pivotal component of innate recognition of viruses, the RIG-I – MAVS – IFN-I axis, is critical in the induction of DC maturation and subsequent cross-priming of CTLs. The adaptor proteins CARD9 and ASC seem to be dispensable in our experimental setup. Given the robust induction of functional CTLs and IFN-I, our data adds to the growing evidence that RIG-I is a promising target to augment cancer therapy especially in combination with ICB.

7. References

[1] T. Mora and A. M. Walczak, “How many different clonotypes do immune repertoires contain?,” *Curr. Opin. Syst. Biol.*, vol. 18, pp. 104–110, 2019.

[2] O. Takeuchi and S. Akira, “Pattern Recognition Receptors and Inflammation,” *Cell*, vol. 140, no. 6, pp. 805–820, Mar. 2010.

[3] R. Medzhitov, “Toll-like receptors and innate immunity,” *Nat. Rev. Immunol.*, vol. 1, no. 2, pp. 135–145, Nov. 2001.

[4] K. Neumann *et al.*, “Clec12a is an inhibitory receptor for uric acid crystals that regulates inflammation in response to cell death,” *Immunity*, vol. 40, no. 3, pp. 389–399, 2014.

[5] D. Sancho *et al.*, “Identification of a dendritic cell receptor that couples sensing of necrosis to immunity,” *Nature*, vol. 458, no. 7240, pp. 899–903, 2009.

[6] T. B. H. Geijtenbeek and S. I. Gringhuis, “Signalling through C-type lectin receptors: Shaping immune responses,” *Nat. Rev. Immunol.*, vol. 9, no. 7, pp. 465–479, 2009.

[7] F. J. Velloso, M. Trombetta-Lima, V. Anschau, M. C. Sogayar, and R. G. Correa, “NOD-like receptors: Major players (and targets) in the interface between innate immunity and cancer,” *Biosci. Rep.*, vol. 29, no. 4, pp. 1–21, 2019.

[8] P. Broz and V. M. Dixit, “Inflammasomes: mechanism of assembly, regulation and signalling.,” *Nat. Rev. Immunol.*, vol. 16, no. 7, pp. 407–420, 2016.

[9] V. Hornung *et al.*, “5′-Triphosphate RNA is the ligand for RIG-I,” *Science (80-.).*, vol. 314, no. 5801, pp. 994–997, 2006.

[10] A. Pichlmair, “RIG-I-Mediated Antiviral Responses to Single-Stranded RNA Bearing 5’-Phosphates,” *Science (80-.).*, vol. 997, no. 2006, 2006.

[11] M. Schlee *et al.*, “Recognition of 5′ Triphosphate by RIG-I Helicase Requires Short Blunt Double-Stranded RNA as Contained in Panhandle of Negative-Strand Virus,” *Immunity*, vol. 31, no. 1, pp. 25–34, Jul. 2009.

[12] H. Poeck *et al.*, “Recognition of RNA virus by RIG-I results in activation of CARD9 and inflammasome signaling for interleukin 1 b production,” *Nat. Immunol.*, vol. 11, no. 1, pp. 63–69, 2010.

[13] R. B. Seth, L. Sun, C. K. Ea, and Z. J. Chen, “Identification and characterization of MAVS, a mitochondrial antiviral signaling protein that

activates NF-κB and IRF3," *Cell*, vol. 122, no. 5, pp. 669–682, 2005.

[14] M. Yoneyama *et al.*, "The RNA helicase RIG-I has an essential function in double-stranded RNA-induced innate antiviral responses," *Nat. Immunol.*, vol. 5, no. 7, pp. 730–737, 2004.

[15] T. Kawai *et al.*, "IPS-1, an adaptor triggering RIG-I- and Mda5-mediated type I interferon induction," *Nat. Immunol.*, vol. 6, no. 10, pp. 981–988, Oct. 2005.

[16] H. Kumar *et al.*, "Essential role of IPS-1 in innate immune responses against RNA viruses," *J. Exp. Med.*, vol. 203, no. 7, pp. 1795–1803, Jul. 2006.

[17] M. Brisse and H. Ly, "Comparative structure and function analysis of the RIG-I-like receptors: RIG-I and MDA5," *Front. Immunol.*, vol. 10, no. JULY, pp. 1–27, 2019.

[18] J. Rehwinkel and M. U. Gack, "RIG-I-like receptors: their regulation and roles in RNA sensing," *Nat. Rev. Immunol.*, 2020.

[19] H. Poeck and J. Ruland, "From virus to inflammation: Mechanisms of RIG-I-induced IL-1β production," *Eur. J. Cell Biol.*, vol. 91, no. 1, pp. 59–64, 2012.

[20] L. L. Lanier, "NK cell recognition," *Annu. Rev. Immunol.*, vol. 23, pp. 225–274, 2005.

[21] J. M. Curtsinger, J. O. Valenzuela, P. Agarwal, D. Lins, and M. F. Mescher, "Cutting Edge: Type I IFNs Provide a Third Signal to CD8 T Cells to Stimulate Clonal Expansion and Differentiation," *J. Immunol.*, vol. 174, no. 8, pp. 4465–4469, 2005.

[22] J. S. Haring, V. P. Badovinac, and J. T. Harty, "Inflaming the CD8+ T Cell Response," *Immunity*, vol. 25, no. 1, pp. 19–29, 2006.

[23] M. F. Mescher *et al.*, "Signals required for programming effector and memory development by CD8+ T cells," *Immunol. Rev.*, vol. 211, pp. 81–92, 2006.

[24] M. E. Keir, L. M. Francisco, and A. H. Sharpe, "PD-1 and its ligands in T-cell immunity," *Curr. Opin. Immunol.*, vol. 19, no. 3, pp. 309–314, 2007.

[25] P. Waterhouse *et al.*, "Lymphoproliferative Disorders with Early Lethality in Mice Deficient in Ctla-4," *Science (80-.).*, vol. 270, no. 5238, pp. 985–988, 2011.

[26] D. R. Leach, M. F. Krummel, and J. P. Allison, "Enhancement of antitumor immunity by CTLA-4 blockade," *Science (80-.).*, vol. 271, no. 5256, pp. 1734–1736, 1996.

[27] F. S. Hodi *et al.*, “Improved Survival with Ipilimumab in Patients with Metastatic Melanoma,” *N. Engl. J. Med.*, vol. 363, no. 8, pp. 711–723, Aug. 2010.

[28] S. L. Topalian *et al.*, “Safety, Activity, and Immune Correlates of Anti–PD-1 Antibody in Cancer,” *N. Engl. J. Med.*, vol. 366, no. 26, pp. 2443–2454, Jun. 2012.

[29] M. Dalod, R. Chelbi, B. Malissen, and T. Lawrence, “Dendritic cell maturation: Functional specialization through signaling specificity and transcriptional programming,” *EMBO Journal*, vol. 33, no. 10. pp. 1104–1116, 2014.

[30] J. Banchereau and R. M. Steinman, “Dendritic cells and the control of immunity.,” *Nature*, vol. 392, no. March, pp. 245–252, 1998.

[31] R. Spörri and C. Reis e Sousa, “Inflammatory mediators are insufficient for full dendritic cell activation and promote expansion of CD4+ T cell populations lacking helper function,” *Nat. Immunol.*, vol. 6, no. 2, pp. 163–170, 2005.

[32] W. R. Heath and J. A. Villadangos, “No driving without a license,” vol. 6, no. 2, pp. 125–126, 2005.

[33] S. R. M. Bennett, F. R. Carbone, F. Karamalis, J. F. A. P. Miller, and W. R. Heath, “Induction of a CD8+ cytotoxic T lymphocyte response by cross-priming requires cognate CD4+ T cell help,” *J. Exp. Med.*, vol. 186, no. 1, pp. 65–70, 1997.

[34] A. Le Bon *et al.*, “Cross-priming of CD8+ T cells stimulated by virus-induced type I interferon,” *Nat. Immunol.*, vol. 4, no. 10, pp. 1009–1015, 2003.

[35] D. Hanahan and R. A. Weinberg, “Hallmarks of cancer: The next generation,” *Cell*, vol. 144, no. 5, pp. 646–674, 2011.

[36] B.-Z. Qian and J. W. Pollard, “Macrophage Diversity Enhances Tumor Progression and Metastasis,” *Cell*, vol. 141, no. 1, pp. 39–51, Apr. 2010.

[37] P. C. Tumeh *et al.*, “PD-1 blockade induces responses by inhibiting adaptive immune resistance,” *Nature*, vol. 515, no. 7528, pp. 568–571, 2014.

[38] S. Woo *et al.*, “STING-Dependent Cytosolic DNA Sensing Mediates Innate Immune Recognition of Immunogenic Tumors,” *Immunity*, vol. 41, no. 5, pp. 830–842, 2014.

[39] J. Galon *et al.*, “Type, density, and location of immune cells within human colorectal tumors predict clinical outcome,” *Science (80-.).*, vol. 313, no. 5795, pp. 1960–1964, 2006.

[40] W. T. Hwang, S. F. Adams, E. Tahirovic, I. S. Hagemann, and G. Coukos, "Prognostic significance of tumor-infiltrating T cells in ovarian cancer: A meta-analysis," *Gynecol. Oncol.*, vol. 124, no. 2, pp. 192–198, 2012.

[41] H. Poeck *et al.*, "5′-triphosphate-siRNA: turning gene silencing and Rig-I activation against melanoma," *Nat. Med.*, vol. 14, no. 11, pp. 1256–1263, 2008.

[42] R. Besch *et al.*, "Proapoptotic signaling induced by RIG-I and MDA-5 results in type I interferon-independent apoptosis in human melanoma cells," *J. Clin. Invest.*, vol. 119, no. 8, pp. 2399–2411, Jul. 2009.

[43] U. Müller *et al.*, "Functional role of type I and type II interferons in antiviral defense," *Science (80-.).*, vol. 264, no. 5167, pp. 1918–1921, 1994.

[44] S. Mariathasan, K. Newton, and D. M. Monack, "Differential activation of the inflammasome by caspase-1 adaptors ASC and Ipaf," vol. 430, no. July, pp. 213–218, 2004.

[45] O. Gross *et al.*, "Card9 controls a non-TLR signalling pathway for innate anti-fungal immunity," *Nature*, vol. 442, no. 7103, pp. 651–656, 2006.

[46] K. Inaba *et al.*, "Generation of Large Numbers of Dendritic Cells from Mouse Bone Marrow Cultures Supplemented with Granulocyte/Macrophage Colony-stimulating Factor," *J. Exp. Med.*, vol. 176, no. December, pp. 1693–1702, 1992.

[47] M. Roederer, "Interpretation of cellular proliferation data: Avoid the panglossian," *Cytom. Part A*, vol. 79 A, no. 2, pp. 95–101, 2011.

[48] M. L. Salem, A. N. Kadima, D. J. Cole, and W. E. Gillanders, "Defining the Antigen-Specific T-Cell Response to Vaccination and Poly(I:C)/TLR3 Signaling," *J. Immunother.*, vol. 28, no. 3, pp. 220–228, May 2005.

[49] H. Negishi *et al.*, "Cross-interference of RLR and TLR signaling pathways modulates antibacterial T cell responses," *Nat. Immunol.*, vol. 13, no. 7, pp. 659–666, 2012.

[50] J. M. M. Den Haan, S. M. Lehar, and M. J. Bevan, "CD8+ but not CD8- dendritic cells cross-prime cytotoxic T cells in vivo," *J. Exp. Med.*, vol. 192, no. 12, pp. 1685–1695, 2000.

[51] H. Singh-Jasuja *et al.*, "The mouse dendritic cell marker CD11c is down-regulated upon cell activation through Toll-like receptor triggering," *Immunobiology*, vol. 218, no. 1, pp. 28–39, 2013.

[52] K. Hoebe *et al.*, “Upregulation of costimulatory molecules induced by lipopolysaccharide and double-stranded RNA occurs by Trif-dependent and Trif-independent pathways,” *Nat. Immunol.*, vol. 4, no. 12, pp. 1223–1229, 2003.

[53] G. R. Stark, I. M. Kerr, B. R. Williams, R. H. Silverman, and R. D. Schreiber, “How cells respond to interferons.,” *Annu. Rev. Biochem.*, vol. 67, pp. 227–64, 1998.

[54] D. B. Stetson and R. Medzhitov, “Recognition of Cytosolic DNA Activates an IRF3-Dependent Innate Immune Response,” *Immunity*, vol. 1, no. January, pp. 93–103, 2006.

[55] H. Ishikawa, Z. Ma, and G. N. Barber, “STING regulates intracellular DNA-mediated, type I interferon-dependent innate immunity,” *Nature*, vol. 461, no. 7265, pp. 788–792, 2009.

[56] K. Hildner *et al.*, “Batf3 deficiency reveals a critical role for CD8α+ dendritic cells in cytotoxic T cell immunity,” *Science (80-.).*, vol. 322, no. 5904, pp. 1097–1100, 2008.

[57] K. Hochheiser *et al.*, “Cutting Edge: The RIG-I Ligand 3pRNA Potently Improves CTL Cross-Priming and Facilitates Antiviral Vaccination,” *J. Immunol.*, vol. 196, no. 6, pp. 2439–2443, 2016.

[58] J. Helft *et al.*, “GM-CSF Mouse Bone Marrow Cultures Comprise a Heterogeneous Population of CD11c+MHCII+ Macrophages and Dendritic Cells,” *Immunity*, vol. 42, no. 6, pp. 1197–1211, Jun. 2015.

[59] D. L. Elion and R. S. Cook, “Harnessing RIG-I and intrinsic immunity in the tumor microenvironment for therapeutic cancer treatment,” *Oncotarget*, vol. 9, no. 48, pp. 29007–29017, 2018.

[60] S. Bek *et al.*, “Targeting intrinsic RIG-I signaling turns melanoma cells into type I interferon-releasing cellular antitumor vaccines,” *Oncoimmunology*, vol. 8, no. 4, pp. 1–9, 2019.

[61] A. M. M. Merad, P. Sathe, J. Helft, J. Miller, “The Dendritic Cell Lineage: Ontogeny and Function of Dendritic Cells and Their Subsets in the Steady State and the Inflamed Setting,” *Annu. Rev. Immunol.*, vol. 41, no. 9, pp. 15–25, 2013.

[62] K. Brasel, T. De Smedt, J. L. Smith, and C. R. Maliszewski, “bone marrow

cultures Generation of murine dendritic cells from flt3-ligand – supplemented bone marrow cultures," *Blood*, vol. 96, no. 9, pp. 3029–3039, 2000.

[63] M. S. Diamond *et al.*, "Type I interferon is selectively required by dendritic cells for immune rejection of tumors," *J. Exp. Med.*, vol. 208, no. 10, pp. 1989–2003, 2011.

[64] A. K. Pinto *et al.*, "Deficient IFN Signaling by Myeloid Cells Leads to MAVS-Dependent Virus-Induced Sepsis," *PLoS Pathog.*, vol. 10, no. 4, 2014.

[65] K. Honda, S. Sakaguchi, C. Nakajima, A. Watanabe, H. Yanai, and M. Matsumoto, "Selective contribution of IFN- a/b signaling to the maturation of dendritic cells induced by double-stranded RNA or viral infection," *PNAS*, 2003.

[66] T. Luft *et al.*, "Type I IFNs enhance the terminal differentiation of dendritic cells.," *J. Immunol.*, vol. 161, no. 4, pp. 1947–53, 1998.

[67] S. Heidegger *et al.*, "RIG-I activating immunostimulatory RNA boosts the efficacy of anticancer vaccines and synergizes with immune checkpoint blockade," *EBioMedicine*, vol. 41, pp. 146–155, 2019.

[68] G. A. Kolumam, S. Thomas, L. J. Thompson, J. Sprent, and K. Murali-Krishna, "Type I interferons act directly on CD8 T cells to allow clonal expansion and memory formation in response to viral infection," *J. Exp. Med.*, vol. 202, no. 5, pp. 637–650, 2005.

[69] M. Cella, F. Facchetti, A. Lanzavecchia, and M. Colonna, "Plasmacytoid dendritic cells activated by influenza virus and CD40L drive a potent TH1 polarization," *Nat. Immunol.*, vol. 1, no. 4, pp. 305–310, 2000.

[70] M. B. Fuertes, S. R. Woo, B. Burnett, Y. X. Fu, and T. F. Gajewski, "Type I interferon response and innate immune sensing of cancer," *Trends in Immunology*, vol. 34, no. 2. Elsevier Ltd, pp. 67–73, 2013.

[71] L. Zitvogel, L. Galluzzi, O. Kepp, M. J. Smyth, and G. Kroemer, "Type I interferons in anticancer immunity," *Nat Rev Immunol*, vol. 15, no. 7, pp. 405–414, 2015.

[72] S. A. Patel and A. J. Minn, "Combination Cancer Therapy with Immune Checkpoint Blockade: Mechanisms and Strategies," *Immunity*, vol. 48, no. 3, pp. 417–433, 2018.

[73] J. W. Huh, J. H. Lee, and H. R. Kim, "Prognostic significance of tumor-infiltrating lymphocytes for patients with colorectal cancer," *Arch. Surg.*, vol.

147, no. 4, pp. 366–371, 2012.

[74] T. F. Gajewski, L. Corrales, J. Williams, B. Horton, A. Sivan, and S. Spranger, “Cancer Immunotherapy Targets Based on Understanding the T Cell-Inflamed Versus Non-T Cell-Inflamed Tumor Microenvironment,” in *Adv Exp Med Biol.*, vol. 176, no. 10, 2017, pp. 19–31.

[75] J. Le Naour, L. Zitvogel, L. Galluzzi, E. Vacchelli, and G. Kroemer, “Trial watch: STING agonists in cancer therapy,” *Oncoimmunology*, vol. 9, no. 1, pp. 1–12, 2020.

[76] Q. Zhu *et al.*, “Cutting Edge: STING Mediates Protection against Colorectal Tumorigenesis by Governing the Magnitude of Intestinal Inflammation,” *J. Immunol.*, vol. 193, no. 10, pp. 4779–4782, 2014.

[77] A. G. Chapuis *et al.*, “T-cell therapy using interleukin-21-primed cytotoxic T-cell lymphocytes combined with cytotoxic T-cell lymphocyte antigen-4 blockade results in long-term cell persistence and durable tumor regression,” *J. Clin. Oncol.*, vol. 34, no. 31, pp. 3787–3795, 2016.

[78] C. Yee and G. A. Lizee, “Personalized therapy tumor antigen discovery for adoptive cellular therapy,” *Cancer J. (United States)*, vol. 23, no. 2, pp. 144–148, 2017.

[79] K. B. Chiappinelli *et al.*, “Inhibiting DNA Methylation Causes an Interferon Response in Cancer via dsRNA Including Endogenous Retroviruses,” *Cell*, vol. 162, no. 5, pp. 974–986, Aug. 2015.

[80] S. Heidegger *et al.*, “RIG-I activation is critical for responsiveness to checkpoint blockade,” *Sci. Immunol.*, vol. 4, no. 39, p. eaau8943, Sep. 2019.

[81] L. Such *et al.*, “Targeting the innate immunoreceptor RIG-I overcomes melanoma-intrinsic resistance to T cell immunotherapy,” *J. Clin. Invest.*, vol. 140, no. 8, pp. 4266–4281, 2020.

[82] D. L. Elion *et al.*, “Therapeutically active RIG-I agonist induces immunogenic tumor cell killing in breast cancers,” *Cancer Res.*, vol. 78, no. 21, pp. 6183–6195, 2018.

[83] X. Jiang *et al.*, “Intratumoral delivery of RIG-I agonist SLR14 induces robust antitumor responses,” *J. Exp. Med.*, vol. 216, no. 12, pp. 2854–2868, 2019.

[84] J. T. Wilson *et al.*, “PH-responsive nanoparticle vaccines for dual-delivery of antigens and immunostimulatory oligonucleotides,” *ACS Nano*, vol. 7, no. 5,

pp. 3912–3925, 2013.

[85] M. Ruzicka *et al.*, “RIG-I-based immunotherapy enhances survival in preclinical AML models and sensitizes AML cells to checkpoint blockade,” *Leukemia*, vol. 34, no. 4, pp. 1017–1026, 2020.

[86] M. R. Middleton *et al.*, “Phase I/II, multicenter, open-label study of intratumoral/intralesional administration of the retinoic acid–inducible gene I (RIG-I) activator MK-4621 in patients with advanced or recurrent tumors,” *Ann. Oncol.*, vol. 29, no. October, p. viii712, 2018.

[87] R. Heidenreich *et al.*, “A novel RNA-based adjuvant combines strong immunostimulatory capacities with a favorable safety profile,” *Int. J. Cancer*, vol. 137, no. 2, pp. 372–384, 2015.

[88] T. Eigentler *et al.*, “Abstract LB-021: Intratumoral RNA-based TLR-7/-8 and RIG-I agonist CV8102 alone and in combination with anti-PD-1 in a Phase I dose-escalation and expansion trial in patients with advanced solid tumors,” *Cancer Res.*, vol. 79, no. 13 Supplement, p. LB-021 LP-LB-021, Jul. 2019.

8. Acknowledgements